

Interpretation of cone penetration tests — a unified approach

P.K. Robertson

Abstract: The electric cone penetration test (CPT) has been in use for over 40 years and is growing in popularity in North America. This paper provides some recent updates on the interpretation of some key geotechnical parameters in an effort to develop a more unified approach. Extensive use is made of the normalized soil behaviour type (SBTn) chart based on normalized cone resistance (Q_t) and normalized friction ratio (F_r). Updates are provided regarding the normalization process and its application to the identification of soil type. The seismic CPT has provided extensive data linking CPT net cone resistance to shear-wave velocity and soil modulus. New correlations are presented in the form of contours of key parameters on the SBTn chart. These new relationships enable a more unified interpretation of CPT results over a wide range of soils. Updates are also provided in terms of in situ state parameter, peak friction angle, and soil sensitivity. The correlations are evaluated using available laboratory and full-scale field test results. Many of the recommendations contained in this paper are focused on low to moderate risk projects where empirical interpretation tends to dominate. For projects where more advanced methods are more appropriate, the recommendations provided in this paper can be used as a screening to evaluate critical regions—zones where selective additional in situ testing and sampling maybe appropriate.

Key words: cone penetration test (CPT), interpretation, soil type, soil modulus, state parameter, peak friction angle, over-consolidation ratio (OCR), sensitivity.

Résumé : L'essai électrique de pénétration au cône (« CPT ») est utilisé depuis plus de 40 ans et sa popularité continue d'augmenter en Amérique du Nord. Cet article présente des mises à jour récentes effectuées pour l'interprétation de quelques paramètres géotechniques clés, ceci dans le but de développer une approche plus unifiée. Les tables des types de comportement de sol normalisées (« SBTn ») sont fréquemment utilisées, ces tables étant basées sur la résistance au cône normalisée (Q_t) et le ratio de friction normalisé (F_r). Des mises à jour sont fournies en lien avec le processus de normalisation et son application à l'identification des types de sols. Le CPT sismique a fourni une grande quantité de données qui ont servi à relier la résistance nette au cône du CPT avec la vitesse des ondes de cisaillement et le module du sol. Les nouvelles corrélations sont représentées sous forme de contours pour les paramètres clés sur les tables de SBTn. Ces nouvelles corrélations permettent d'obtenir une interprétation plus unifiée des résultats des CPT pour un éventail plus complet de types de sols. Les mises à jour sont aussi données en termes de l'état in situ des paramètres, de l'angle de friction maximal et de la sensibilité du sol. Les corrélations sont évaluées à l'aide de résultats d'essais en laboratoire et sur le terrain à grande échelle. Plusieurs recommandations présentées dans cet article visent les projets à risque faible à modéré dans lesquels les interprétations sont surtout empiriques. Pour les projets qui nécessitent des méthodes d'analyse plus avancées, les recommandations présentées dans l'article peuvent servir d'ébauche pour établir les régions ou zones critiques qui auraient avantage à être échantillonnées in situ et investiguées de façon plus poussée.

Mots-clés : essai de pénétration au cône (« CPT »), interprétation, type de sol, module du sol, paramètre d'état, angle de friction maximal, rapport de surconsolidation (« OCR »), sensibilité.

[Traduit par la Rédaction]

Introduction

The electric cone penetration test (CPT) has been in use for over 40 years. The CPT has major advantages over traditional methods of field site investigation, such as drilling

and sampling, because it is fast, repeatable, and economical. In addition, it provides near-continuous data and has a strong theoretical background. These advantages have led to a steady increase in the use and application of the CPT in North America and many other places around the world. In 1983, Robertson and Campanella published two major papers on the interpretation of the CPT (Robertson and Campanella 1983a, 1983b). Since 1983, there have been several major publications on the interpretation of the CPT (Lunne et al. 1997; Mayne 2007). Because of the growing use and experience with the CPT, the author felt that it was appropriate to provide an update on certain aspects of CPT interpretation. This paper will not provide a complete background on the use and interpretation of the CPT, as this has been covered by others (e.g., Lunne et al. 1997; Mayne 2007). The main objective of this paper is to focus

Received 17 June 2008. Accepted 27 May 2009. Published on the NRC Research Press Web site at cgj.nrc.ca on 10 November 2009.

P.K. Robertson.¹ University of Alberta Geotechnical Centre, Department of Civil and Environmental Engineering, University of Alberta, 3-133 Markin/CNRL Natural Resources Engineering Facility, Edmonton, AB T6G 2W2, Canada.

¹Present address: Gregg Drilling & Testing Inc., California, 2726 Walnut Ave., Signal Hill, CA 90755, USA (e-mail: probertson@greggdrilling.com).

on certain aspects that link CPT interpretation to soil type in a more unified manner. In an effort to present this unified interpretation approach, most of the suggested empirical correlations will be presented as contours on the normalized soil behaviour type (SBT) chart, first suggested by Robertson (1990).

Significant developments have occurred in both the theoretical and experimental understanding of the CPT penetration process and the influence of various soil parameters. These developments have illustrated that real soil behaviour is often complex and difficult to accurately capture in a simple soil model. Hence, semi-empirical correlations still tend to dominate in CPT practice although most are well supported by theory.

The original Robertson and Campanella (1983a, 1983b) publications and also the book by Lunne et al. (1997) divided the interpretations of the CPT into those that relate to either drained cone penetration (i.e., coarse-grained soils) or undrained cone penetration (i.e., fine-grained soils). This approach will be continued in this paper, although the goal will be to integrate the two into a more complete system.

Role of CPT in geotechnical practice

Hight and Leroueil (2003) suggested that the appropriate level of sophistication for a site characterization program should be based on the following criteria:

- Precedent and local experience.
- Design objectives.
- Level of geotechnical risk.
- Potential cost savings.

The evaluation of geotechnical risk was described by Robertson (1998) and is dependent on the hazards (what can go wrong), probability of occurrence (how likely is it to go wrong), and consequences (what are the outcomes).

For low-risk projects, in situ logging tests (e.g., CPT) and index testing on disturbed samples combined with conservative design criteria are often appropriate. For moderate-risk projects, the above can be supplemented with additional specific in situ testing, such as seismic cone penetration tests with pore-pressure measurements (SCPTu) and field vane shear tests (VST) combined with selective sampling and basic laboratory testing to develop site-specific correlations. For high-risk projects, the above can be used for screening to identify potentially critical regions–zones appropriate to the design objectives. This should be followed by selective high-quality sampling and advanced laboratory testing. The results of the laboratory testing should be correlated to the in situ test results to apply the results to other regions of the project.

A common complaint about the CPT is that it does not provide a soil sample. Although it is correct that a soil sample is not normally obtained during the CPT, most commercial CPT operators also carry simple push-in soil samplers that can be pushed using the CPT installation equipment to obtain a small (typically 25 mm diameter) disturbed soil sample of similar size to that obtained from the standard penetration test. The preferred approach and often more cost-effective solution is to obtain a detailed continuous stratigraphic profile using the CPT, then to move over a short distance (<1 m) and push a small diameter soil sam-

pler to obtain discrete selective soil samples in critical layers–zones that were identified by the CPT. The push rate to obtain the soil sample can be significantly faster than the 2 cm/s required for the CPT and sampling can be rapid and cost effective for a small number of discrete samples.

Many of the recommendations contained in this paper are focused on low- to moderate-risk projects where traditional methods are appropriate and where empirical interpretation tends to dominate. For projects where more advanced methods are more appropriate, the recommendations provided in this paper can be used as a screening to evaluate critical regions–zones where selective additional in situ testing and sampling may be appropriate.

Equipment and procedures

Lunne et al. (1997) provided a detailed description on developments in CPT equipment, procedures, checks, corrections, and standards, which will not be repeated here. Most CPT systems today include pore-pressure measurements (i.e., CPTu) and provide CPT results in digital form. The addition of shear-wave velocity (Robertson et al. 1986b) is also becoming increasingly popular (i.e., SCPTu). Hence, it is now more common to see the combination of cone resistance (q_c), sleeve friction (f_s), penetration pore pressure (u), and sometimes, shear-wave velocity (V_s) measured in one profile. The addition of shear-wave velocity has provided valuable insight into correlations between cone resistance and soil modulus that will be discussed in a later section.

There are several major issues related to equipment design and procedure that are worth repeating and updating. It is now common that cone pore pressures are measured behind the cone in what is referred to as the u_2 position (ISSMFE 1999; ASTM 2000). In this paper, it will be assumed that the cone pore pressures are measured in the u_2 position. Due to the inner geometry of the cone, the ambient pore water pressure acts on the shoulder behind the cone and on the ends of the friction sleeve. This effect is often referred to as the unequal end-area effect (Campanella et al. 1982). Many commercial cones now have equal end-area friction sleeves that essentially remove the need for any correction to f_s and hence, provide more reliable sleeve friction values. However, the unequal end-area effect is always present for the cone resistance q_c and there is a need to correct q_c to the corrected total cone resistance, q_t .

This correction is insignificant in sands, as q_c is large relative to the water pressure u_2 and hence, $q_t \sim q_c$ in coarse-grained soils (i.e., sands). It is still common to see CPT results in terms of q_c in coarse-grained soils. However, the unequal end-area correction can be significant in soft fine-grained soil where q_c is low relative to the high water pressure around the cone due to the undrained penetration process. It is now common to see CPT results corrected for unequal end-area effects and presented in the form of q_t , f_s , and u_2 , especially in softer soils. The correlations presented in this paper will be in terms of the corrected cone resistance, q_t , although in sands q_c can be used as a replacement.

Although pore-pressure measurements are becoming more common with the CPT (i.e., CPTu), the accuracy and precision of the cone pore-pressure measurements for onshore testing are not always reliable and repeatable due to loss of

saturation of the pore-pressure element. At the start of each CPTu sounding, the porous element and sensor are saturated with a viscous liquid, such as silicon oil or glycerin (Campanella et al. 1982). However, for an onshore CPTu, the cone is often required to penetrate several metres through unsaturated soil before reaching saturated soil. If the unsaturated soil is either clay or dense silty sand, the suction in the unsaturated soil can be sufficient to desaturate the cone pore-pressure sensor. The use of viscous liquids, such as silicon oil, has minimized the loss of saturation, but has not completely removed the problem. Although it is possible to pre-punch or pre-drill the sounding and fill the hole with water, few commercial CPT operators carry out this procedure if the water table is more than a few metres below the ground surface. A further complication is that when a cone is pushed through saturated dense silty sand or very stiff over-consolidated clay, the pore pressure measured in the u_2 position can become negative due to the dilatancy of the soil in shear, resulting in small air bubbles coming out of solution in the cone sensor pore fluid and loss of saturation in the sensor. If the cone is then pushed through a softer fine-grained soil where the penetration pore pressures are high, these air bubbles can go back into solution and the cone becomes saturated again. However, it takes time for these air bubbles to go into solution, which can result in a somewhat sluggish pore-pressure response for several metres of penetration. Hence, it is possible for a cone pore-pressure sensor to alternate from saturated to unsaturated several times in one sounding. Although this appears to be a major problem with the measurement of pore pressure during a CPTu, it is possible to obtain good pore-pressure measurements in suitable ground conditions where the ground water level is close to the surface and the ground is predominately soft. CPTu pore-pressure measurements are almost always reliable in offshore testing due to the high ambient water pressure that ensures full saturation. It is interesting to note that when the cone is stopped and a pore-pressure dissipation test performed below the ground water level, any small air bubbles in the cone sensor tend to go back into solution (during the dissipation test) and the resulting equilibrium pore pressure can be accurate, even when the cone may not have been fully saturated during penetration before the dissipation test.

Although pore-pressure measurements can be less reliable than the cone resistance for onshore testing, it is still recommended that pore-pressure measurements be made for the following reasons: any correction to q_t for unequal end-area effects is better than no correction in soft fine-grained soils, dissipation test results provide valuable information regarding the equilibrium piezometric profile, and penetration pore pressures provide a qualitative evaluation of drainage conditions during the CPT and also assist in evaluating soil behaviour type.

Figure 1 shows a comparison between two CPTus carried out only 1 m apart, and illustrates excellent repeatability in terms of both cone resistance and friction ratio ($R_f = f_s/q_c$ %). CPT-04 was carried out using silicon oil and CPT-03 used glycerin as the saturating fluid. The groundwater level was at a depth of about 1.8 m. Both soundings provided similar penetration pore pressures down to about 7 m. After penetration through dense sand at a depth of 6.5 m, CPT-03 recorded negative pore pressures that resulted in a somewhat

slower response for the next few metres, after which the response of the two soundings are again similar. At a depth of 8.5 m, the measured pore pressure in CPT-03 is only 33% of the more accurate pore pressure from CPT-04. If only CPT-03 was carried out, it would be difficult to recognize the error in the u_2 measurement. This profile illustrates that although q_t and f_s can be repeatable, the penetration pore pressures may not always be repeatable throughout the full CPT sounding.

Although Fig. 1 shows excellent repeatability for the sleeve friction measurement, it has been documented (e.g., Lunne et al. 1986) that the CPT sleeve friction is generally less accurate than the cone tip resistance. The lack of accuracy in f_s measurements is primarily due to the following factors (Lunne and Andersen 2007):

- Pore pressure effects on the ends of the sleeve.
- Tolerance in dimensions between the cone and sleeve.
- Surface roughness of the sleeve.
- Load cell design and calibration.

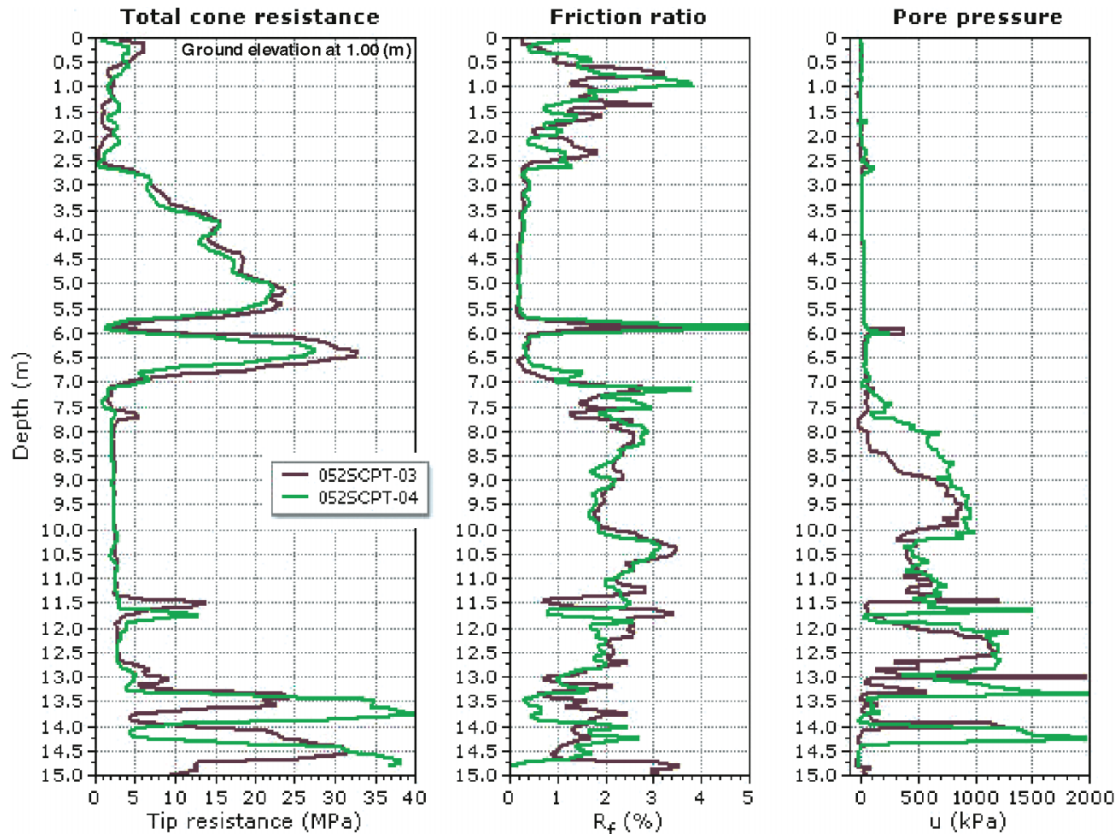
ASTM standard D5778 (ASTM 2000) specifies the use of an equal end-area friction sleeve to minimize the pore-pressure effects. All standards have strict limits on dimensional tolerances. The “International reference test procedure for CPT” (IRTP) (ISSMFE 1999) has clear specifications on surface roughness. This author prefers a cone design with an independent sleeve friction load cell in compression for improved accuracy. ASTM standard D5778 (ASTM 2000) and the IRTP (ISSMFE 1999) specify zero-load readings before and after each sounding for improved accuracy. With good quality control it is possible to obtain repeatable sleeve friction measurements, as shown in Fig. 1. However, f_s measurements, in general, will be less accurate than tip resistance in most soft fine-grained soils.

Throughout this paper, use will be made of the normalized soil behaviour type (SBTn) chart using normalized CPT parameters. Hence, accuracy in both q_t and f_s are important, particularly in soft fine-grained soil. Accuracy in f_s measurements requires that the CPT be carried out according to the standard (e.g., ASTM D5778) with particular attention to details on tolerances, zero-load readings, and the use of equal end-area friction sleeves.

Soil type

One of the major applications of the CPT has been the determination of soil stratigraphy and the identification of soil type. This has been accomplished using charts that link cone parameters to soil type. Early charts using q_c and friction ratio (R_f) were proposed by Douglas and Olsen (1981), but the charts proposed by Robertson et al. (1986a) and Robertson (1990) have become very popular (e.g., Long 2008). Robertson et al. (1986a) and Robertson (1990) stressed that the CPT-based charts were predictive of soil behaviour type (SBT), because the cone responds to the in situ mechanical behaviour of the soil and not directly to soil classification criteria based on grain-size distribution and soil plasticity (e.g., Unified Soil Classification System, USCS (ASTM 2006)). Grain-size distribution and Atterberg limits are measured on disturbed soil samples. Fortunately, soil classification criteria based on grain-size distribution and plasticity often relate reasonably well to in situ soil behaviour

Fig. 1. Comparison between two adjacent CPTu soundings. (Note: CPT-03 glycerin; CPT-04, silicon oil.)



and hence, there is often good agreement between USCS-based classification and CPT-based SBT (e.g., Molle 2005). However, several examples can be given when differences can arise between USCS-based soil types and CPT-based SBT. For example, a soil with 60% sand and 40% fines may be classified as “silty sand” (sand–silt mixtures) or “clayey sand” (sand–clay mixtures) using the USCS. If the fines have high clay content with high plasticity, the soil behaviour may be more controlled by the clay and the CPT-based SBT will reflect this behaviour and will predict a more clay-like behaviour, such as “silt mixtures – clayey silt to silty clay” (Robertson 1990, SBT zone 4). If the fines are nonplastic, soil behaviour will be controlled more by the sand and the CPT-based SBT would predict a more sand-like soil type, such as “sand mixtures – silty sand to sandy silt” (SBT zone 5). Very stiff, heavily overconsolidated fine-grained soils tend to behave more like a coarse-grained soil in that they tend to dilate under shear and can have high undrained shear strength compared with their drained strength and can have a CPT-based SBT in either zone 4 or 5. Soft, saturated low-plastic silts tend to behave more like clays in that they have low undrained shear strength and can have a CPT-based SBT in zone 3 (clays – clay to silty clay). These few examples illustrate that the CPT-based SBT may not always agree with traditional USCS-based soil types based on samples and that the biggest difference is likely to occur in the mixed soils region (i.e., sand mixtures and silt mixtures). Geotechnical engineers are often more interested in the in situ soil behaviour than a classification based only on grain-size distribution and plasticity

carried out on disturbed samples, although knowledge of both is helpful.

Robertson (1990) proposed using normalized (and dimensionless) cone parameters, Q_{t1} , F_r , and B_q , where

$$[1] \quad Q_{t1} = (q_t - \sigma_{vo}) / \sigma'_{vo}$$

$$[2] \quad F_r = [f_s / (q_t - \sigma_{vo})] 100\%$$

$$[3] \quad B_q = (u_2 - u_0) / (q_t - \sigma_{vo}) = \Delta u / (q_t - \sigma_{vo})$$

where σ_{vo} is the in situ total vertical stress, σ'_{vo} is the in situ effective vertical stress, u_0 is the in situ equilibrium water pressure, and Δu is the excess penetration pore pressure.

In the original paper by Robertson (1990) the normalized cone resistance was defined using the term Q_t . The term Q_{t1} is used here to show that the cone resistance is the corrected cone resistance, q_t , and the stress exponent for stress normalization is 1.0 (further details are provided in a later section).

In general, the normalized charts provide more reliable identification of SBT than the non-normalized charts, although when the in situ vertical effective stress is between 50 to 150 kPa there is often little difference between normalized SBT (referred to as SBTn in this paper) and non-normalized SBT. The above normalization was based on theoretical work by Wroth (1984). Robertson (1990) suggested two charts based on either Q_{t1} – F_r and Q_{t1} – B_q , but recommended that the Q_{t1} – F_r chart was generally more reliable.

Since 1990 there have been other CPT soil behaviour-type charts developed (e.g., Jefferies and Davies 1991; Olsen and Mitchell 1995; Eslami and Fellenius 1997). The chart by Eslami and Fellenius (1997) is based on non-normalized parameters using effective cone resistance, $q_c (= q_t - u_2)$, and f_s . The effective cone resistance, q_c , suffers from lack of accuracy in soft fine-grained soils, as will be discussed in a later section. Zhang and Tumay (1999) developed a CPT-based soil classification system based on fuzzy logic where the results are presented in the form of percentage soil type (e.g., percentage; clay, silt, and sand size). Because the CPT responds to soil behaviour, it would appear more logical to predict soil behaviour type (SBT) rather than grain-size distribution, although for many soils the two will be similar.

Conceptually, any normalization to account for increasing stress should also account for the important influence of horizontal effective stresses, as penetration resistance is strongly influenced by the horizontal effective stresses (Jamiolkowski and Robertson 1988). However, this continues to have little practical benefit for most projects without a prior knowledge of in situ horizontal stresses. Even normalization using only vertical effective stress requires some input of soil unit weight and groundwater conditions. Fortunately, commercial software packages have increasingly made this easier and unit weights estimated from the non-normalized SBT charts (Robertson et al. 1986a) appear to be reasonably effective for many applications (Lunne et al. 1997).

Jefferies and Davies (1991) proposed a modified SBTn chart that incorporates the pore pressure directly into a modified normalized cone resistance using $Q_{t1}(1 - B_q)$. Recently, Jefferies and Been (2006) updated their modified chart using the parameter $Q_{t1}(1 - B_q) + 1$, to overcome the problem in soft sensitive soils where $B_q > 1$.

Jefferies and Been (2006) noted that

$$[4] \quad Q_{t1}(1 - B_q) + 1 = (q_t - u_2)/\sigma'_{vo}$$

Hence, the parameter $Q_{t1}(1 - B_q) + 1$ is simply the effective cone resistance, $(q_t - u_2)$, normalized by the vertical effective stress. Although incorporating pore pressure into the normalized cone resistance is conceptually attractive, it has practical problems. Accuracy is a major concern in soft fine-grained soils where q_t is small compared with u_2 . Hence, the difference $(q_t - u_2)$ is very small and lacks accuracy and reliability in most soft soils. For most commercial cones, the precision of Q_{t1} in soft fine-grained soils is about $\pm 20\%$; whereas, the precision for $Q_{t1}(1 - B_q) + 1$ is about $\pm 40\%$, due to the combined lack of precision in $(q_t - u_2)$. Loss of saturation further complicates this parameter, as illustrated in Fig. 1.

Jefferies and Davies (1993) identified that a soil behaviour type index, I_c , could represent the SBTn zones in the $Q_{t1}-F_r$ chart, where I_c is essentially the radius of concentric circles that define the boundaries of soil type. Robertson and Wride (1998) modified the definition of I_c to apply to the Robertson (1990) $Q_{t1}-F_r$ chart, as defined by

$$[5] \quad I_c = [(3.47 - \log Q_{t1})^2 + (\log F_r + 1.22)^2]^{0.5}$$

Contours of I_c are shown in Fig. 2 on the Robertson

(1990) $Q_{t1}-F_r$ SBTn chart. The contours of I_c can be used to approximate the SBT boundaries. Jefferies and Davies (1993) suggested that the SBT index I_c could also be used to modify empirical correlations that vary with soil type. This is a powerful concept and has been used where appropriate in this paper.

The form of eq. [5] and the shape of the contours of I_c in Fig. 2 illustrate that I_c is not overly sensitive to the potential lack of accuracy of the sleeve friction, f_s , but is more controlled by the more accurate tip stress, q_t . Research (e.g., Long 2008) has sometimes questioned the reliability of the SBT based on sleeve friction values (e.g., $Q_{t1}-F_r$ charts). However, numerous studies (e.g., Molle 2005) have shown that the normalized charts based on $Q_{t1}-F_r$ provide the best overall success rate for SBT compared with samples. It can be shown, using eq. [5], that if f_s varies by as much as $\pm 50\%$, the resulting variation in I_c is generally less than $\pm 10\%$. For soft soils, that falls within the lower part of the $Q_{t1}-F_r$ chart (e.g., $Q_{t1} < 20$); I_c is insensitive to f_s .

Robertson and Wride (1998) and the update by Zhang et al. (2002) suggested a normalized cone parameter with a variable stress exponent, n , where

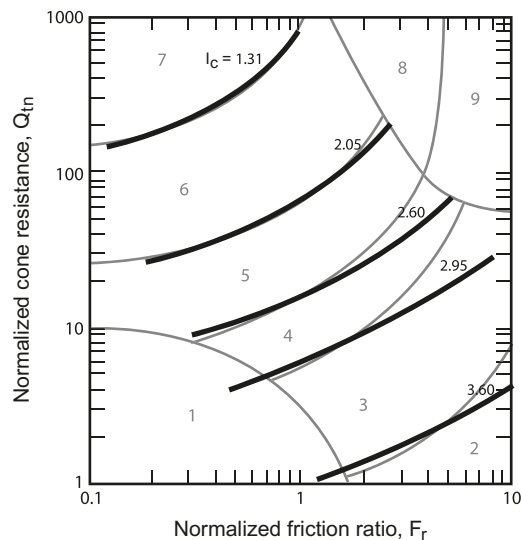
$$[6] \quad Q_{tn} = [(q_t - \sigma_{vo})/p_a](p_a/\sigma'_{vo})^n$$

where $(q_t - \sigma_{vo})/p_a$ is the dimensionless net cone resistance, $(p_a/\sigma'_{vo})^n$ is the stress normalization factor, p_a is atmospheric pressure in the same units as q_t and σ_{vo} , and n is the stress exponent that varies with SBTn. Note that when $n = 1$, $Q_{tn} = Q_{t1}$. Zhang et al. (2002) suggested that the stress exponent, n , could be estimated using the SBTn index, I_c , and that I_c should be defined using Q_{tn} .

In recent years there have been several publications regarding the appropriate stress normalization (Olsen and Malone 1988; Boulanger and Idriss 2004; Moss et al. 2006; Cetin and Isik 2007). The contours of the stress exponent suggested by Cetin and Isik (2007) are very similar to those by Zhang et al. (2002). Idriss and Boulanger (2004) suggested that the stress exponent should vary with relative density, where the exponent is close to 1.0 in loose sands and less than 0.5 in dense sands. The contours by Moss et al. (2006) are similar to those first suggested by Olsen and Malone (1988). All the above methods agree that in the clean sand region of the SBTn chart, the stress exponent is typically close to 0.5 and in the clay region, the stress exponent is close to 1.0. Only the SBTn chart suggested by Jefferies and Davies (1991) uses a stress normalization of $n = 1.0$ throughout. As this is a key point for the interpretation of the CPT results over a wide range of soil types, a more detailed discussion will be provided.

The cone penetration resistance (q_t) is a measure of the shear strength of the soil. In normally consolidated clay, the undrained shear strength increases linearly with increasing vertical effective stress. Hence, the cone resistance (q_t) also increases linearly with increasing vertical effective stress and Wroth (1984) showed that in fine-grained soils the appropriate stress exponent is $n = 1.0$. In coarse-grained soils, it is well established that the shear strength envelope in terms of shear stress versus effective stress for all but very loose soils is curved over a wide stress range. This curvature was described by Vesic and Clough (1968) and Bolton (1986). Large calibration chamber studies, and more re-

Fig. 2. Contours of soil behaviour type index, I_c (thick lines), on normalized SBTn $Q_{tn}-F_r$ chart. (SBT zones based on Robertson (1990).)



cently centrifuge tests with sands at a constant relative density, have also shown that the cone resistance in coarse-grained soils increases nonlinearly with increasing vertical effective stress. The average stress exponent to capture this change with vertical stress is typically close to $n = 0.5$ (Baldi et al. 1989). The nonlinearity is more pronounced in dense sands than in loose sands (i.e., the stress exponent n is larger in loose sands).

Bolton (1986) represented the curvature of the strength envelope by showing that the secant peak friction angle decreases with increasing effective stress, and that the friction angle is essentially constant for very loose sands and is often referred to as the constant volume friction angle (ϕ_{cv}) or critical state friction angle (ϕ_{cs}). Hence, Bolton implied that the stress exponent should be close to 1.0 in very loose sands and in dense sands at very high stresses where dilatancy is suppressed and grain crushing occurs. Therefore, the stress exponent (n) for cone resistance should tend toward 1.0 as sand behaviour becomes more contractive (i.e., dilatancy becomes suppressed) and grain crushing becomes more pronounced. The stress level at which grain crushing is predominant and the peak friction angle becomes constant is a function of grain characteristics. Rounded uniform silica sands do not experience significant grain crushing until a mean effective stress at failure of around 2 MPa (Bolton 1986); whereas, angular silica sands and silty sands can reach this level at mean effective stresses less than 1 MPa. Crushable sands, such as carbonate sands, can reach this level at a mean effective stress closer to 0.1 MPa. Hence, the stress level at which crushing becomes significant is a function of soil compressibility. The stresses close to the cone during penetration in dense sands can be close to these high values and grain crushing is occurring close to the cone. However, within the sphere of influence around the cone, the average effective stress to fail the sand is not as high as the cone resistance and grain crushing is not occurring everywhere.

Boulanger (2003) showed that a generalized critical state line (CSL) can be developed based on Bolton's (1986) rela-

tionship. The generalized CSL presented by Boulanger (2003) clearly shows that the CSL (in void ratio – log effective stress space) is almost flat at low mean effective confining stresses (less than 2 atmospheres (200 kPa)) and eventually becomes steep (and similar to that for clays) at very high stresses. A similar curved CSL was confirmed by Jefferies and Been (2006). When the slope of the CSL is very small, there is a strong link between relative density and state parameter. Wroth (1984) showed that a stress normalization for cone resistance using $n = 1$ is appropriate when the normally consolidated line is essentially parallel with the CSL. However, in sands, the CSL is clearly nonlinear over a wide stress range and the consolidation lines vary relative to the CSL. Hence, it would appear that critical-state soil mechanics would support the concept of a variable stress exponent to normalize penetration resistance and that the stress exponent can be around 0.5 at low stresses and tending toward 1.0 at high stresses when the CSL line becomes straight and the consolidation line for sands becomes parallel to the CSL.

Jefferies and Been (2006) showed that the slope of the CSL was a measure of the compressibility of the soil and that there is a link between the slope of the CSL and the SBTn index, I_c . It is therefore possible to estimate soil compressibility and hence, the stress level at which the stress exponent tends toward a value of 1.0 using the CPT SBTn index, I_c .

Based on the previous discussion, the following is recommended to allow for a variation of the stress exponent with both SBTn I_c and effective overburden stress using

$$[7] \quad n = 0.381(I_c) + 0.05(\sigma'_{vo}/p_a) - 0.15$$

where $n \leq 1.0$.

The proposed updated contours of n (for $\sigma'_{vo}/p_a = 1.0$) are shown in Fig. 3. Figure 3 shows that for most fine-grained soils, the stress exponent will be 1.0. The stress exponent will range from 0.5 to 0.9 for most coarse-grained soils when in situ vertical stresses are not high. The region where $n = 1.0$ moves up the chart with increasing confining stress. When the in situ vertical effective stress is greater than 1MPa, the stress exponent will be essentially 1.0 for most soils.

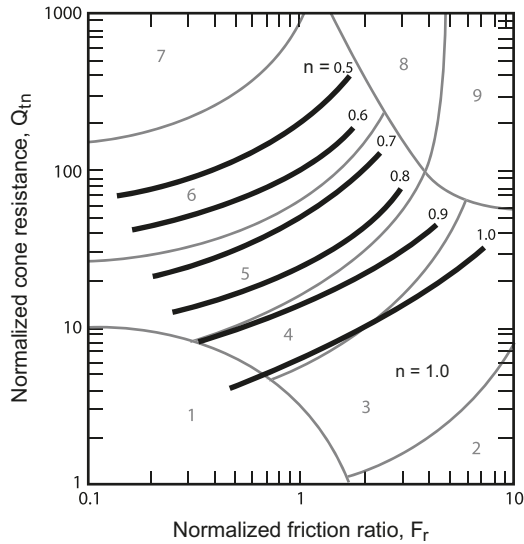
The above recommended normalization is not an arbitrary approach, but is based on experimental observations designed to improve correlations with various geotechnical parameters.

Caution should be used when comparing CPT-based SBT to samples with traditional classification systems based only on grain-size distribution and plasticity. Factors such as changes in stress history, in situ stresses, macro fabric, void ratio, and water content will also influence the CPT response and resulting SBT. The manner in which the excess pore pressures dissipate during a pause in the cone penetration can significantly aid in identifying the soil type.

Stratigraphy — transition zones

Robertson and Campanella (1983a) discussed how the cone tip resistance is influenced by the soil ahead and behind the cone tip. Ahmadi and Robertson (2005) illustrated this using numerical analyses and confirmed that the cone

Fig. 3. Contours of stress exponent, n (thick lines), (for $\sigma'_{vo}/p_a = 1.0$) on normalized SBTn $Q_{tn}-F_r$ chart.



can sense a soil interface up to 15 cone diameters ahead and behind, depending on the strength–stiffness of the soil and the in situ effective stresses. In strong–stiff soils, the zone of influence is large (up to 15 cone diameters), whereas in soft soils the zone of influence is rather small (as small as one cone diameter). Ahmadi and Robertson (2005) showed that the size of the zone of influence decreased with increasing stress (e.g., dense sands behave more like loose sand at high values of effective stress).

The zone of influence ahead and behind a cone during penetration will influence the cone resistance at any interface (boundary) between two soil types of significantly different strength and stiffness. Hence, it is often important to identify transitions between different soil types to avoid possible misinterpretation. This issue has become increasingly important with software that provides interpretation of every data point from the CPT. When CPT data are collected at close intervals (typically every 20 to 50 mm) several data points are “in transition” when the cone passes an interface between two different soil types (e.g., from sand to clay and vice versa). It is possible to identify the transition from one soil type to another using the rate of change of I_c . When the CPT is in transition from sand to clay, the SBTn I_c will move from low values in the sand to higher values in the clay. Robertson and Wride (1998) suggested that the approximate boundary between sand-like and clay-like behaviour is around $I_c = 2.60$. Hence, when the rate of change of I_c is rapid and is crossing the boundary defined by $I_c = 2.60$, the cone is likely in transition from a sand-like to clay-like soil or vice versa. Profiles of I_c can provide a simple means to identify and remove these transition zones.

Drained CPT penetration — coarse-grained soils (cohesionless)

The following section is focused on coarse-grained soils where the penetration process is essentially drained and where most of the geotechnical parameters are based on drained behaviour.

Stiffness (modulus)

Eslaamizaad and Robertson (1997) and Mayne (2000) have shown that the load settlement response for both shallow and deep foundations can be accurately predicted using the measured shear-wave velocity, V_s . Although direct measurement of V_s is preferred over estimates, relationships with cone resistance are useful for smaller low-risk projects, where V_s measurements are not always taken. Schneider et al. (2004) showed that V_s in sands is controlled by the number and area of grain-to-grain contacts, which in turn depend on relative density, effective stress state, rearrangement of particles with age, and cementation. Penetration resistance in sands is also controlled by relative density, effective stress state, and to a lesser degree by age and cementation. Thus, although strong relationships between V_s and penetration resistance exist, some variability should be expected. There are many existing relationships between cone resistance and V_s (or small strain shear modulus, G_0), but most were developed for either sands or clays and generally relatively young deposits. The accumulated 20 years of experience with SCPT results enables updated relationships between cone resistance and V_s to be developed for a wide range of soils, using the CPT SBTn chart ($Q_{tn}-F_r$) as a base. As V_s is a direct measure of the small strain shear modulus, G_0 , there can also be improved linkages between CPT results and soil modulus.

Based on over 100 SCPT profiles from 22 sites in California combined with published data, a set of contours of normalized shear-wave velocity, V_{s1} , (Robertson et al. 1992) was developed on the normalized SBT $Q_{tn}-F_r$ chart, as shown in Fig. 4, where

$$[8] \quad V_{s1} = V_s(p_a/\sigma'_{vo})^{0.25} \quad (\text{in m/s})$$

As the CPT measurements are normalized in terms of Q_{tn} and F_r , the resulting shear-wave velocity values are also normalized. The characteristics of the more than 1000 CPT– V_s data pairs are summarized in Table 1. The deposits ranged predominately from the Holocene to Pleistocene age and were mostly uncemented, although cementation was possible in some soils. Andrus et al. (2007) showed that most Holocene-age deposits have V_{s1} values less than 250 m/s. In general, the Holocene-age data tends to plot in the center-left portion of the SBTn chart, whereas the Pleistocene-age data tends to plot in the center-right portion of the chart. There was significant scatter in the data pairs, due in part to the variation in depth interval over which the readings were taken. Typically, CPT measurements are taken every 5 cm, whereas V_s measurements are taken every 1 to 1.5 m. Part of the scatter may also be due to uncertainty with respect to age and cementation for these natural deposits.

The contours of V_{s1} in Fig. 4 can be approximated using the following equations (both in m/s):

$$[9] \quad V_{s1} = (\alpha_{vs}Q_{tn})^{0.5}$$

or

$$[10] \quad V_s = [\alpha_{vs}(q_t - \sigma_v)/p_a]^{0.5}$$

where α_{vs} is the shear-wave velocity cone factor.

Fig. 4. Contours of normalized shear-wave velocity, V_{s1} (thick lines), on normalized SBTn Q_{tn} - F_r chart for uncemented Holocene- and Pleistocene-age soils. $V_{s1} = V_s(p_a/\sigma'_{vo})^{0.25}$ (m/s).

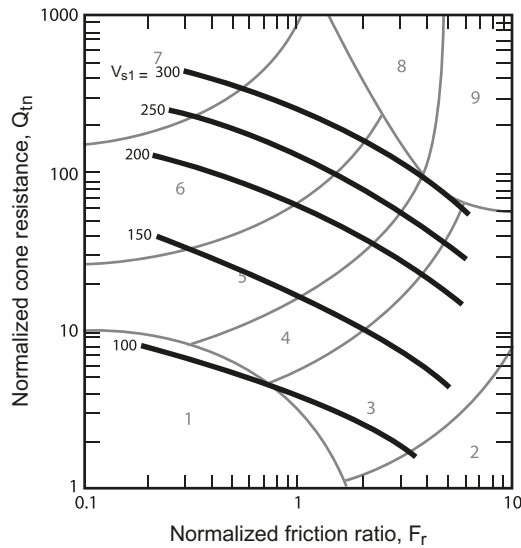


Table 1. Characteristic values of CPT- V_s database.

	Q_{tn}	F_r (%)	V_{s1} (m/s)	σ'_{vo} (kPa)
Maximum	577	13.13	906	580
Minimum	0.67	0.15	72	19
Average	59	3.13	260	190

Note: Total number of data pairs = 1035.

As the contour shapes for α_{vs} are similar to those for I_c , α_{vs} can be estimated using

$$[11] \quad \alpha_{vs} = 10^{(0.55I_c + 1.68)} \quad (\text{in } (m/s)^2)$$

The contours shown in Fig. 4 were further evaluated and verified using additional published data from other regions of the world (e.g., Schnaid 2005; Andrus et al. 2007).

Hegazy and Mayne (1995) proposed a relationship between shear-wave velocity and cone resistance as a function of friction ratio. Andrus et al. (2007) suggested a similar relationship for combined Holocene- and Pleistocene-age deposits based on 229 data pairs from California, South Carolina, and Japan. Andrus et al. (2007) suggested a correction factor based on age of the deposit to improve the correlation. Typically, Pleistocene-age soils had V_{s1} values 25% higher than Holocene-age soils. Knowledge of soil age would improve the correlations, but often the age of the deposit is not always known in advance for most small low-risk projects. Hence, the general relationship shown in Fig. 4 and eq. [9] is recommended for most Holocene- to Pleistocene-age deposits. The predicted shear-wave velocity using eq. [10] in Pleistocene-age deposits may be somewhat underestimated. The effectiveness of the proposed relationship will be evaluated further in a later section.

At low shear strain levels (less than about $10^{-4}\%$), the shear modulus in soils is constant and has a maximum value, G_0 . This small strain shear modulus is determined from the shear-wave velocity using the equation

$$[12] \quad G_0 = \rho V_s^2$$

where ρ is the mass density (or total unit weight divided by the acceleration of gravity) of the soil.

Using the V_s contours, Fig. 5 shows the associated contours of the small strain shear modulus number, K_G , where

$$[13] \quad G_0 = K_G p_a (\sigma'_{vo}/p_a)^n$$

where n is a stress exponent that has a value of about 0.5 for most coarse-grained soils.

Previous research (Seed and Idriss 1970; Hardin and Drnevich 1972) showed that the modulus number, K_G , can vary from 400 to 1600 in young, uncemented, loose to dense sand. These values agree well with the range shown in Fig. 5.

Relationships between soil modulus and cone resistance can have the general form

$$[14] \quad G_0 = \alpha_G (q_t - \sigma_{vo})$$

where α_G is the shear modulus factor for estimating the small strain shear modulus (G_0) from net cone resistance ($q_t - \sigma_{vo}$).

As the stress exponent is similar for the normalization of both Q_{tn} and G_0 in the sand region, it follows that

$$[15] \quad \alpha_G = K_G/Q_{tn}$$

Hence, it is possible to develop contours of α_G that are also shown in Fig. 5. Although the stress normalization for Q_{tn} varies from the sand to clay region, the error in extending the contours of α_G into the clay region is small. Eslaamizaad and Robertson (1997) showed that for young, uncemented sands, the ratio of G_0/q_t (i.e., α_G) varied with normalized cone resistance. Table 2 shows the approximate range of values from Eslaamizaad and Robertson (1997). These values compare well with the values shown in Fig. 5, because in sands $q_t \sim (q_t - \sigma_{vo})$ and $0.1\% < F_r < 3\%$.

Robertson and Campanella (1989) showed that the ratio G_0/q_t varied from 20 to 125 for variations in the overconsolidation ratio (OCR) and soil plasticity for clays. These values are also consistent with the range shown in Fig. 5. Robertson (1995) showed that the value of G_0/q_t varied from 2 to 100 as Q_{tn} changed from 1000 to 1, which is also consistent with Fig. 5.

Eslaamizaad and Robertson (1996a) and Schnaid (2005) showed that it is possible to identify cemented soils using the ratio of G_0/q_t . Hence, if the measured $G_0/(q_t - \sigma_{vo})$ (i.e., α_G) is significantly larger than estimated using Fig. 5, the soils are likely cemented.

It is also possible to estimate the appropriate value of α_G from I_c based on the link with α_{vs} using

$$[16] \quad \alpha_G = (\rho/p_a)\alpha_{vs}$$

where (ρ/p_a) is in units of (s/m)².

For an average unit weight $\gamma = 18 \text{ kN/m}^3$ ($\rho = 1.84$), it follows that

$$[17] \quad \alpha_G = 0.0188 [10^{(0.55I_c + 1.68)}]$$

Hence, the small strain shear modulus, G_0 , for young, uncemented soils can be estimated using

Fig. 5. Contours of small strain shear modulus number, K_G , and modulus factor, α_G , on normalized SBTn Q_{tn} - F_r chart for uncemented Holocene- and Pleistocene-age soils. $G_0 = K_G P_a (\sigma'_{vo}/p_a)^{0.50}$; $G_0 = \alpha_G (q_t - \sigma_{vo})$.

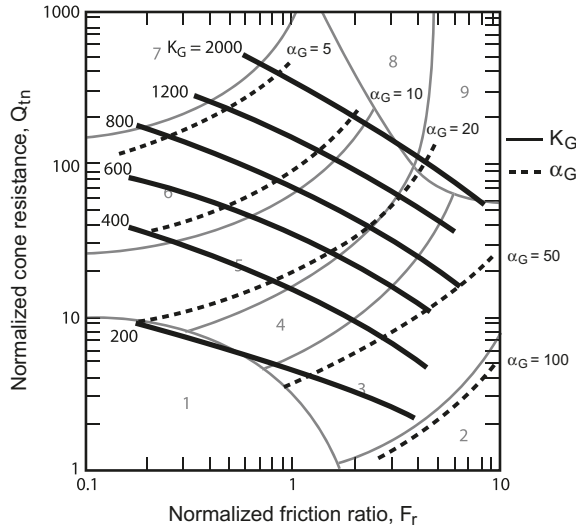


Table 2. Typical G_0/q_t values for sands suggested by Eslaamizaad and Robertson (1997).

Normalized cone resistance, Q_{tn}	Ratio G_0/q_t
500	2 to 4
100	5 to 10
20	15 to 30

$$[18] \quad G_0 = 0.0188 [10^{(0.55I_c + 1.68)}] (q_t - \sigma_{vo})$$

Figure 5 and eq. [18] provide a simplified means to estimate the small strain shear modulus over a wide range of soils using CPT data. The relationships shown in Figs. 4 and 5 are less reliable in the region for fine-grained soils (i.e., when $I_c > 2.60$), as the sleeve friction f_s and hence F_r , are strongly influenced by soil sensitivity. The relationships are generally better in the coarse-grained region (i.e., when $I_c < 2.60$) and are primarily for uncemented, predominately silica-based soils of Holocene and Pleistocene age.

For some applications, engineers require an estimate of the Young's modulus, E' , which is linked to the shear modulus via

$$[19] \quad E' = 2(1 + \nu)G$$

where ν is Poisson's ratio, which ranges from 0.1 to 0.3 for most soils under drained conditions, and G is shear modulus. Hence, for most coarse-grained soils, $E' \sim 2.5G$.

As the small strain shear modulus, G_0 , applies only at very small strains, there is a need to soften G_0 to a strain level appropriate for design purposes. Eslaamizaad and Robertson (1997) showed that the amount of softening required for design was a function of the degree of loading. Fahey and Carter (1993) suggested a simple approach to estimate the amount of softening using

$$[20] \quad G/G_0 = 1 - f(q/q_{ult})^g$$

where q is the applied load (e.g., net bearing pressure for

foundations), q_{ult} is the ultimate or failure load (e.g., ultimate bearing capacity for foundations), q/q_{ult} is the degree of loading, and f and g are constants depending on soil type and stress history.

Fahey and Carter (1993) and Mayne (2005) suggested that values of $f = 1$ and $g = 0.3$ are appropriate for uncemented soils that are not highly structured. For a degree of loading from 0.2 to 0.3, the ratio G/G_0 ranges from 0.30 to 0.38. Hence, for many design applications the appropriate Young's modulus for application in simplified elastic solutions is approximately

$$[21] \quad E' \sim 0.8G_0$$

Using this ratio, it is possible to create contours of Young's modulus number, K_E , on the CPT SBTn chart as shown in Fig. 6, where

$$[22] \quad E' = K_E p_a (\sigma'_{vo}/p_a)^n$$

where n is a stress exponent that has a value of about 0.5 for most coarse-grained soils.

As the application of Young's modulus, E' , is generally only applicable to drained soils, the contours on Fig. 6 are therefore limited to the region defined by $I_c < 2.60$.

Some existing relationships between soil modulus and cone resistance have the form

$$[23] \quad E' = \alpha_E (q_t - \sigma_{vo})$$

where α_E is the modulus factor for estimating Young's modulus (E') from net cone resistance ($q_t - \sigma_{vo}$). Most existing relationships use q_c , whereas they should be using $(q_t - \sigma_{vo})$, although the error is generally small in sands, where $q_t \gg \sigma_{vo}$ and $q_c \sim (q_t - \sigma_{vo})$.

As the stress exponent is similar for the normalization of both Q_{tn} and E' in the sand region, it follows that

$$[24] \quad \alpha_E = K_E/Q_{tn}$$

Hence, it is possible to develop contours of α_E that are also shown in Fig. 6.

Combining eqs. [18] and [21], it is possible to estimate the appropriate value of α_E from I_c using the following equation:

$$[25] \quad \alpha_E = 0.015 [10^{(0.55I_c + 1.68)}]$$

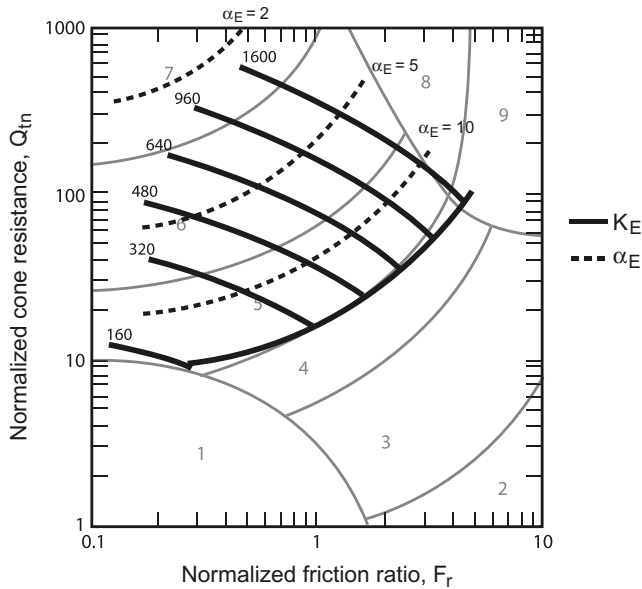
From this, the Young's modulus, E' , for uncemented, predominately silica-based soils of either Holocene or Pleistocene age (when $I_c < 2.60$) can be estimated using

$$[26] \quad E' = 0.015 [10^{(0.55I_c + 1.68)}] (q_t - \sigma_{vo})$$

Bellotti et al. (1989) showed that the ratio E'/q_c varied between 3 and 12 for aged, normally consolidated sands and between 5 and 20 for overconsolidated sands and was a function of normalized cone resistance. The relationship shown in Fig. 6 indicates that a more appropriate ratio should be $E'/(q_t - \sigma_{vo})$ and that the range shown in Fig. 6 is consistent with previous work.

Figure 6 and eq. [26] provide a simplified means to estimate the equivalent Young's modulus using CPT data for a wide range of coarse-grained soils. As the appropriate value

Fig. 6. Contours of Young’s modulus number, K_E , and modulus factor, α_E , on normalized SBTn $Q_{tn}-F_r$ chart for uncemented Holocene- and Pleistocene-age soils. $E' = K_E P_a (\sigma'_{vo}/p_a)^{0.50}$; $E' = \alpha_E (q_t - \sigma_{vo})$.



for E' is a function of the degree of loading, it is also possible to vary α_E as a function of degree of loading. The values of α_E shown in Fig. 6 are for an average degree of loading of about 0.25 (i.e., factor of safety around 4). As the degree of loading increases, the associated value of α_E will decrease. To incorporate degree of loading into the estimate of E' , the final form would be

$$[27] \quad E' = 0.047 [1 - (q/q_{ult})^{0.3}] [10^{(0.55I_c + 1.68)}] (q_t - \sigma_{vo})$$

For low-risk projects, the simpler form shown in eq. [26] would generally be adequate.

Recent full-scale footing tests (Briaud and Gibbens 1999; Anderson et al. 2007) provide an opportunity to evaluate the above correlation for E' in sandy soils. Briaud and Gibbens (1999) describe several full-scale tests carried out on 3 m by 3 m footings tested at the Texas A & M University test site. The site is composed of about 11 m of sand over clay shale with groundwater at about 5 m. The sands are of the Eocene age and are lightly cemented and overconsolidated. The average net cone resistance, $(q_t - \sigma_{vo})$, below the footing to a depth of about 7 m was 7.5 MPa and the average SBT index, I_c was 1.7 ($Q_{tn} = 120$, $F_r = 0.7\%$). Based on Fig. 4 and eq. [9], the estimated normalized shear-wave velocity is 220 m/s. The measured shear-wave velocity in the upper 7 m was about 210 m/s, which at an average vertical effective stress of about 50 kPa is a normalized shear-wave velocity of 250 m/s. The predicted normalized shear-wave velocity based on the CPT is slightly smaller than the measured value, which is consistent with the age and cementation of this deposit. The measured ultimate failure load for the 3 m square footing was about 10 MN (i.e., $q_{ult} = 1.1$ MPa). The predicted ultimate bearing stress based on the CPT and the average cone resistance beneath the footing ($q_{t(av)}$) using $q_{ult} = 0.16q_{t(av)}$ (Eslaamizaad and Robertson 1996b) is 1.2 MPa. Eslaamizaad and Robertson (1997) and Mayne

(2000) showed that the load settlement response was well predicted using the measured shear-wave velocity profile at the test site. As the predicted shear-wave velocity is close to the measured value, the suggested approach would also give a good but slightly conservative prediction of the measured load settlement.

Anderson et al. (2007) describe a full-scale test on a 1.8 m diameter, 0.6 m thick concrete footing embedded 0.6 m below ground surface over a deposit of silty sand in Florida. Groundwater was 1.7 m below ground surface and the footing was loaded statically to a footing pressure of 222 kPa. The CPT correctly identified that the soil down to a depth of about 5.7 m is composed of sand to silty sand becoming finer with depth. At a depth of 2.5 m there is a thin layer of soft sandy silt. The average normalized cone resistance, Q_{tn} , in the silty sand was 225 in the upper 1.5 m, decreasing to 25 at a depth of 2.5 m then increasing to about 150 at a depth of 3.7 m, then decreasing to 50 from 4.3 to 5.0 m. The average normalized friction ratio, F_r , varied from 0.4% to 0.8% to a depth of about 5.0 m. From a depth of about 1.5 to 5.0 m, the SBT index I_c varied from 1.3 to 2.0. The estimated average normalized shear-wave velocity to a depth of 5.0 m was about 200 m/s. Based on the measured normalized CPT parameters and the suggested correlation for E' , the predicted settlement under a footing pressure of 222 kPa is 5.5 mm compared with the measured settlement of 2.5 mm. Anderson et al. (2007) applied a total of 22 different methods to predict the settlement, of which the best one gave a prediction of 5.59 mm with an average value of 14.4 mm. The proposed CPT-based correlation predicts a settlement closer to the measured value, but slightly conservative. The evaluation of settlement may have been further improved if shear-wave velocity measurements were included in the field tests.

In situ state

Robertson and Campanella (1983a) showed that the evaluation of the in situ state in terms of relative density is not very reliable due to variations in compressibility for sands. Sands with high compressibility produce lower cone resistance for the same relative density compared with sands with low compressibility. The compressibility of sands is controlled by grain characteristics, such as grain mineralogy and angularity (e.g., carbonate sands are more compressible than silica sands and angular silica sands are more compressible than rounded silica sands). The evaluation of relative density is also influenced by the age and stress history of the sand (Kulhawy and Mayne 1990).

Based on critical-state concepts, Jefferies and Been (2006) provide a detailed description of the evaluation of the soil state using the CPT. They describe in detail that the inverse problem of evaluating the state from CPT response is complex and depends on several soil parameters. The main parameters are essentially the shear stiffness, shear strength, compressibility, and plastic hardening. Jefferies and Been (2006) provide a description of how the state can be evaluated using a combination of laboratory and in situ tests. They stress the importance of determining the in situ horizontal effective stress and shear modulus using in situ tests and determining the shear strength, compressibility, and plastic hardening parameters from laboratory testing on re-

constituted samples. They also show how the inverse problem can be assisted using numerical modeling. For high-risk projects, a detailed interpretation of CPT results using laboratory results and numerical modeling can be appropriate (e.g., Shuttle and Cuning 2007), although soil variability can complicate the interpretation procedure. For low-risk projects and in the initial screening for high-risk projects, there is a need for a simple estimate of the soil state. Plewes et al. (1992) provided a means to estimate the soil state using the normalized SBT chart suggested by Jefferies and Davies (1991). Jefferies and Been (2006) updated this approach using the normalized SBT chart based on the parameter $Q_{t1}(1 - B_q) + 1$. As this author has concerns about the accuracy and precision of the Jefferies and Been (2006) normalized parameter in soft soils, a similar approach can be developed using the normalized SBTn $Q_{tn}-F_r$ chart. The contours of state parameter ψ suggested by Plewes et al. (1992) and Jefferies and Been (2006) were based primarily on calibration chamber results for sands. When the state parameter approach is applied to clays, there is a link between the state parameter and the OCR.

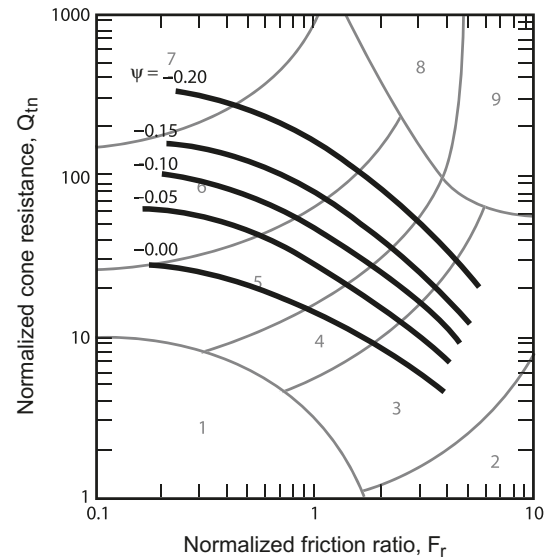
Based on the data presented by Jefferies and Been (2006) and Shuttle and Cuning (2007) as well the measurements from the CANLEX project (Wride et al. 2000) for predominately coarse-grained uncemented young soils, combined with the link between the OCR and state parameter in fine-grained soil, Fig. 7 shows estimated contours of state parameter ψ on the updated SBTn $Q_{tn}-F$ chart for uncemented Holocene-age soils. The contours shown in Fig. 7 are approximate, as the stress state and plastic hardening will also influence the estimate of the in situ soil state in the coarse-grained region of the chart (i.e., when $I_c < 2.60$) and soil sensitivity for fine-grained soils. An area of uncertainty in the approach used by Jefferies and Been (2006) is the use of Q_{t1} rather than Q_{tn} . Figure 7 uses Q_{tn} as it is believed that this form of normalized parameter has a wider application, although this issue may not be fully resolved for some time.

Shear strength

Based on calibration chamber results, Robertson and Campanella (1983a) showed that the peak friction angle (ϕ'_p) for clean, uncemented silica sands could be estimated from the normalized cone resistance. Kulhawy and Mayne (1990) updated the relationship based on a larger database.

Jefferies and Been (2006) showed that the state parameter is strongly linked to the peak friction angle through soil dilatancy. Using the average relationship between the state parameter and peak friction angle suggested by Jefferies and Been (2006) and the contours of the state parameter shown in Fig. 7, it is possible to generate approximate contours of the peak friction angle on the SBTn $Q_{tn}-F_r$ chart, as shown in Fig. 8. For comparison, the values of Q_{tn} for various values of the peak friction angle based on Kulhawy and Mayne (1990) are also shown in Fig. 8. The values of the peak friction angle based on the state parameter are similar to those suggested by Kulhawy and Mayne (1990) in the region $1.8 < I_c < 2.2$. However, the shape of the contours may partially explain why some published comparisons (e.g. Mayne 2007) between CPT results and laboratory-derived friction angles may not always agree with the empirical correlations

Fig. 7. Contours of estimated state parameter, ψ (thick lines), on the normalized $Q_{tn}-F_r$ chart for uncemented Holocene-age soils.



by either Robertson and Campanella (1983a) or Kulhawy and Mayne (1990). Note that as the friction ratio (F_r) increases (and hence, soil compressibility increases) the normalized cone resistance (Q_{tn}) decreases for a constant peak friction angle. This is consistent with observations of high values of ϕ'_p in compressible sands with relatively low values of cone resistance, as found, for example, in carbonate sands. The contours of ϕ'_p will likely move up slightly at high values of F_r due to aging and (or) cementation effects.

Undrained CPT penetration — fine-grained soils

The following section focuses on fine-grained soils where the penetration process is essentially undrained and where most of the geotechnical parameters are based on undrained behaviour. In fine-grained soils, it is common to use the normalized cone resistance, Q_{t1} . However, based on the earlier discussion, when $I_c > 2.60$, $Q_{t1} = Q_{tn}$; hence, the more general term Q_{tn} will be used in this section.

In situ state

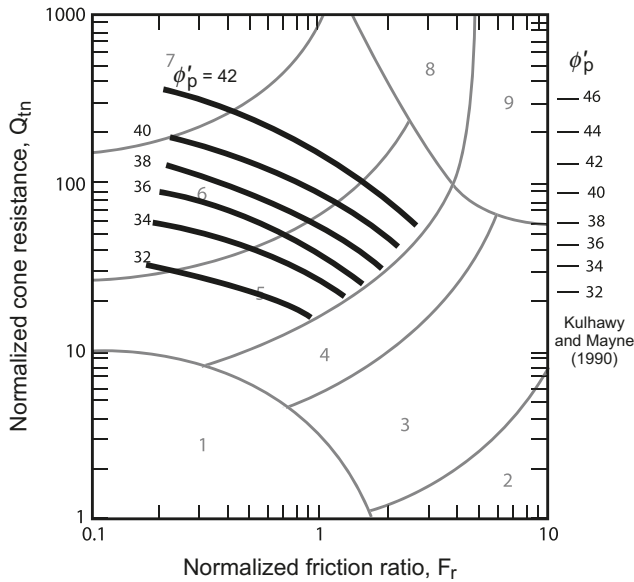
For fine-grained soils, the in situ state is usually defined in terms of OCR, where the OCR is defined as the ratio of the maximum past effective consolidation stress and the present effective overburden stress

$$[28] \quad \text{OCR} = \frac{\sigma'_p}{\sigma'_{vo}}$$

For mechanically overconsolidated soils where the only change has been the removal of the overburden stress, this definition is appropriate. However, for cemented and (or) aged soils, the OCR may represent the ratio of the yield stress and the present effective overburden stress. The yield stress will depend on the direction and type of loading.

The most common method to estimate the OCR and yield stress in fine-grained soils was suggested by Kulhawy and Mayne (1990)

Fig. 8. Contours of peak friction angle, ϕ'_p (thick lines), on normalized $Q_{tn}-F_r$ chart for uncemented Holocene-age sandy soils.



$$[29] \quad OCR = k \left(\frac{q_t - \sigma_{vo}}{\sigma'_{vo}} \right) = kQ_{tn}$$

or

$$[30] \quad \sigma'_p = k(q_t - \sigma_{vo})$$

where k is the preconsolidation cone factor and σ'_p is the preconsolidation or yield stress.

An average value of $k = 0.33$ can be assumed, with an expected range of 0.2 to 0.5. The higher values of k are recommended in aged, heavily overconsolidated clays. If previous experience is available in the same deposit, the values of k should be adjusted to reflect this experience and to provide a more reliable profile of the OCR. Estimates of the OCR using eq. [29] are not strongly influenced by soil sensitivity, as the range of values for k does not vary greatly. This topic will be discussed further in a later section.

Undrained shear strength ratio (s_u/σ'_{vo})

Application of the undrained strength ratio (s_u/σ'_{vo}) can be useful since this relates directly to the OCR. Critical-state soil mechanics presents a relationship between the undrained shear strength ratio for normally consolidated fine-grained soil under different directions of loading and the effective stress friction angle, ϕ' (Ohta et al. 1985).

For normally consolidated fine-grained soil, the undrained shear strength ratio ranges from 0.2 to 0.3 (Jamiolkowski et al. 1985) with an average value of 0.22 in direct simple shear; hence, it is often reasonable to assume

$$[31] \quad (s_u/\sigma'_{vo})_{NC} = 0.22$$

in direct simple shear, where the subscript NC represents normally consolidated.

The peak undrained shear strength ratio can be estimated using

$$[32] \quad (s_u/\sigma'_{vo}) = \left(\frac{q_t - \sigma_{vo}}{\sigma'_{vo}} \right) (1/N_{kt}) = Q_{tn}/N_{kt}$$

where N_{kt} is a cone factor that varies from about 10 to 20, with an average of 14.

Hence, for the general value of $N_{kt} = 14$

$$[33] \quad (s_u/\sigma'_{vo}) = Q_{tn}/14$$

For a normally consolidated fine-grained soil where $(s_u/\sigma'_{vo})_{NC} = 0.22$ and $N_{kt} = 14$, $(Q_{tn})_{NC} = 3.08$ with a range from 2 to 6.

Lunne et al. (1997) and others have shown that the sleeve friction values are often similar to the remolded undrained shear strength of fine-grained soils. Figure 9 shows an example of a comparison between the remolded undrained shear strength measured using the field vane test and the measured CPT sleeve friction at Scoggins Dam (Farrar et al. 2008). Good agreement was obtained between the sleeve friction measurements and the remolded undrained shear strength. Lunne et al. (1997) correctly caution that in very sensitive soft clays, the small remolded strength can result in very low sleeve friction values with an inherent loss of accuracy. Based on the assumption that the sleeve friction (f_s) measures the remolded shear strength of the soil (i.e., $s_{u(r)} = f_s$), the remolded undrained shear strength ratio is given by

$$[34] \quad s_{u(r)}/\sigma'_{vo} = f_s/\sigma'_{vo} = (F_r Q_{tn})/100$$

By combining eqs. [33] and [34], soil sensitivity, S_t , can also be estimated using

$$[35] \quad S_t = s_u/s_{u(r)} = 7.1/F_r$$

where the constant (7.1 in eq. [35]) varies from about 5 to 10 with an average of about 7.1. This is similar to the value of 7.5 suggested by Rad and Lunne (1986) using the non-normalized friction ratio (R_f) and the value of 7.3 suggested by Mayne (2007).

Based on eq. [34], it is possible to represent approximate contours of $(s_{u(r)}/\sigma'_{vo})$ on the normalized SBTn chart, as shown in Fig. 10. Note that as sensitivity increases, the contours move toward region 1, which is identified as “sensitive fine-grained soils”. The contours of $(s_{u(r)}/\sigma'_{vo})$ are presented as a guide, as any lack of accuracy in sleeve friction measurements will influence the result.

As shown in eq. [32], the normalized cone resistance for normally consolidated clay $(Q_{tn})_{NC}$ is in the range 2 to 6 with an average of 3.08. Hence, for insensitive normally consolidated fine-grained soil the normalized cone value (Q_{tn}) ranges between 2 and 6 and falls on or close to the contour for $(s_{u(r)}/\sigma'_{vo}) = 0.22$, as shown in Fig. 10. As sensitivity increases, the cone factor (N_{kt}) decreases slightly (Lunne et al. 1997). Hence, values of Q_{tn} also decrease slightly as sensitivity increases. This variation is illustrated by the arrow in Fig. 10 that shows how normalized cone values Q_{tn} and F_r vary with sensitivity for a normally consolidated fine-grained soil. Values of sensitivity (for normally consolidated soils, OCR = 1.0) are also shown on the contours in Fig. 10.

For insensitive ($S_t = 1.0$) fine-grained soils, it is also possible to identify contours of the OCR using eq. [29] and as-

Fig. 9. Comparison between CPT sleeve friction and field vane remolded undrained shear strengths, Scoggins Dam (adapted from Farrar et al. 2008).

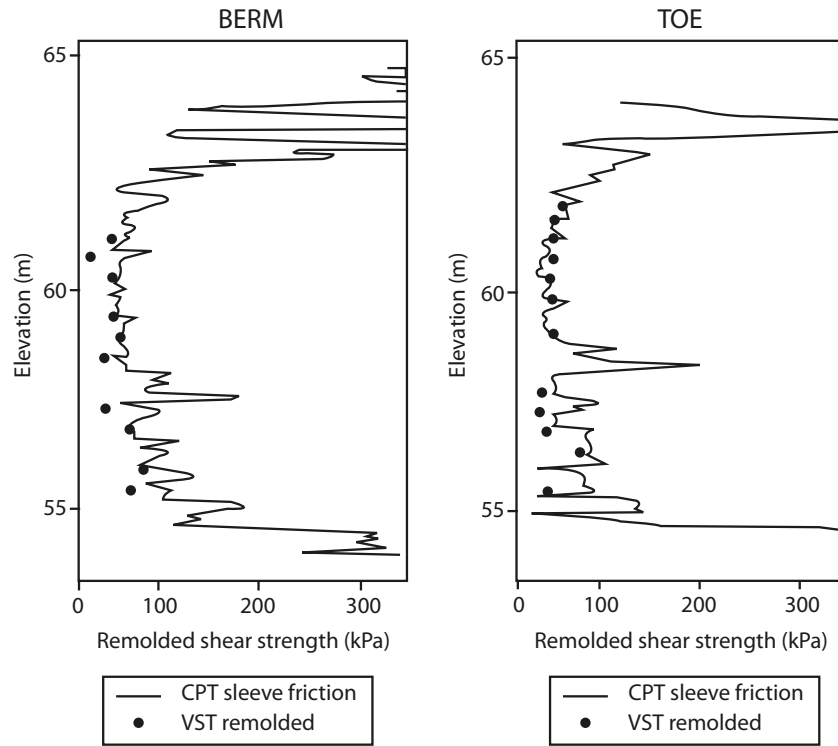
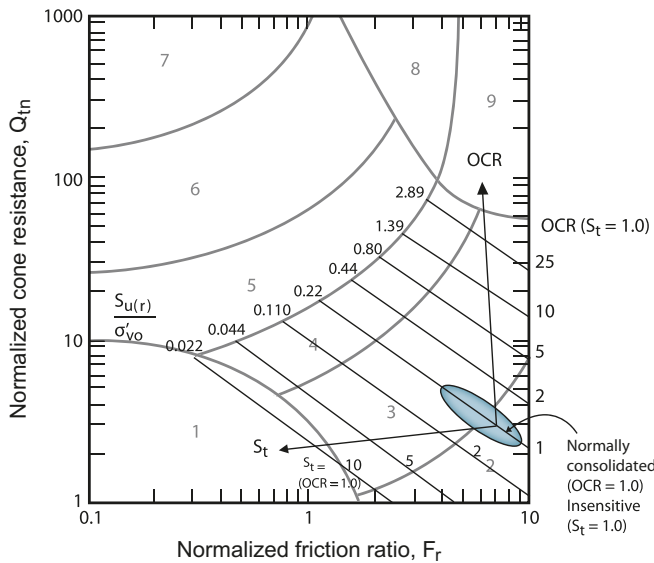


Fig. 10. Contours of remolded undrained shear strength ratio ($s_{u(r)}/\sigma'_{vo}$) plus trends in the OCR and soil sensitivity on normalized $Q_{tn}-F_r$ chart.



suming $s_{u(r)} = s_u$, as shown in Fig. 10. It is possible to include an arrow that shows how normalized cone values vary with OCR for insensitive fine-grained soil. Figure 10 clearly shows that the normalized cone values, Q_{tn} and F_r , in most natural soils, are functions of both the OCR and soil sensitivity (S_t).

The challenge for engineers is to separate the influence of sensitivity and the OCR from the measured values of normalized cone resistance. Figure 10 shows that Q_{tn} is not

strongly influenced by soil sensitivity, which explains why estimates of the undrained shear strength ratio and the OCR from Q_{tn} are generally quite reliable. Likewise, F_r is not strongly influenced by the OCR, but is more controlled by soil sensitivity. Based on these observations and the fact that N_{kt} is close to 14 for many insensitive fine-grained soils, the following simplified approach to estimate sensitivity and peak undrained strength ratio in direct simple shear is recommended:

$$[36] \quad S_t = 7.1/F_r$$

$$[37] \quad (s_u/\sigma'_{vo}) = Q_{tn}/N_{kt} \quad (\text{where initial } N_{kt} = 14)$$

If the estimated sensitivity is high, the undrained strength ratio should be modified using smaller values for N_{kt} . If CPT pore-pressure measurements are made, the normalized parameter B_q can also be used to estimate N_{kt} , as suggested by Lunne et al. (1997). For sensitive clays ($S_t > 10$), the value of f_s (and hence F_r) can be very low with an inherent loss in accuracy. Hence, the estimate of sensitivity should be used only as a guide. The field vane shear test (VST) can be used to verify soil sensitivity, where appropriate. An alternate but similar approach is to first estimate the OCR via Q_{tn} (eq. [29]), then estimate the undrained strength ratio via the OCR using relationships based on critical-state soil mechanics to account for direction of loading (Mayne 2008).

For larger, moderate- to high-risk projects, where additional high quality field and laboratory data may be available, site-specific correlations should be developed based on consistent and relevant values of both s_u and the OCR.

Constrained modulus, M

Consolidation settlements (at the end of primary consolidation) can be estimated using the one-dimensional (1-D) constrained tangent modulus, M , (Lunne et al. 1997) where

$$[38] \quad M = 1/m_v = \delta\sigma_v/\delta\varepsilon = 2.3(1 + e_0)\sigma'_{vo}/C_{c/r}$$

where m_v is the equivalent oedometer coefficient of compressibility, $\delta\sigma_v$ is the change in vertical stress, $\delta\varepsilon$ is the change in vertical strain, e_0 is the initial void ratio, and $C_{c/r}$ is the compression index, either C_c or C_r , depending on σ'_{vo} .

Mayne (2007) has shown that the ratio of M/G_0 varies from 0.02 to 2 for soft clays to sands. Using the link between normalized cone values and G_0 as a starting point, it is possible to develop contours of the constrained modulus number, K_M , on the normalized soil behaviour type (SBTn) chart, $Q_{tn}-F_r$, as shown in Fig. 11, where

$$[39] \quad M = K_M p_a (\sigma'_{vo}/p_a)^a$$

where a is a stress exponent.

Janbu (1963) showed that the stress exponent (a) was equal to 1.0 for stresses above the preconsolidation stress and zero below the preconsolidation stress (i.e., M is approximately constant below the preconsolidation stress). Hence, at stresses less than the preconsolidation stress

$$[40] \quad M = K_M p_a$$

The flat dilatometer test (DMT) has often been shown to provide excellent estimates of settlement using predicted values of the 1-D constrained modulus (Monaco et al. 2006). The shape and location of the contours of K_M were guided by recent correlations between normalized DMT and CPT parameters (Robertson 2009). The shape of the contours was also guided by existing relationships between M and net cone resistance ($q_t - \sigma_{vo}$).

Existing correlations between constrained modulus and cone resistance typically have the form

$$[41] \quad M = \alpha_M (q_t - \sigma_{vo})$$

where α_M is the constrained modulus cone factor.

Sanglerat (1972) suggested that α_M varies with soil plasticity and natural water content for a wide range of fine-grained and organic soils, although the data were based on q_c . Mayne (2007) showed that α_M varied with soil type and net cone resistance with values from 1 to 10, where the low values apply to soft clays.

Based on the contours shown in Fig. 11 and eq. [41], the following simplified correlation is suggested.

When $I_c > 2.2$ use

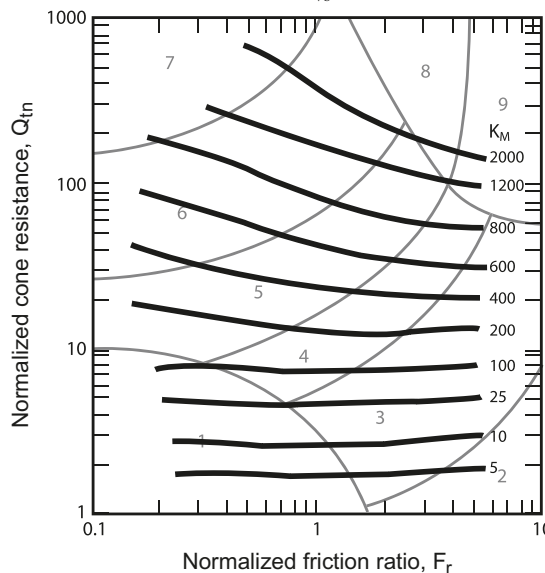
$$[42] \quad \begin{aligned} \alpha_M &= Q_{tn} & \text{when } Q_{tn} \leq 14 \\ \alpha_M &= 14 & \text{when } Q_{tn} > 14 \end{aligned}$$

When $I_c < 2.2$ use

$$[43] \quad \alpha_M = 0.03 [10^{(0.55I_c + 1.68)}]$$

Equation [42] shows that when $Q_{tn} \leq 14$, α_M varies from about 2 to 14, which is similar to that observed by Mayne (2007), but there is a clearer link on how to select the appropriate value for α_M .

Fig. 11. Contours of 1-D constrained modulus number, K_M , on normalized $Q_{tn}-F_r$ chart. $M = K_M p_a (\sigma'_{vo}/p_a)^a$.



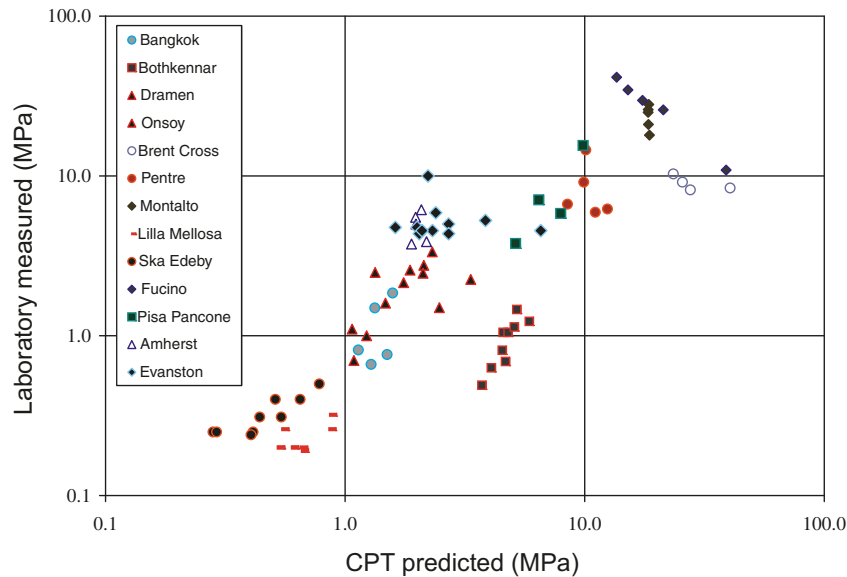
To evaluate the suggested correlation for M for relatively soft, fine-grained soils (clays), where $Q_{tn} \leq 14$, results from an unpublished database (courtesy of P. Mayne, Georgia Institute of Technology (Georgia Tech), Atlanta, Ga., 2008) of CPT and laboratory results from 13 major clay sites around the world were used and the results presented in Fig. 12. Figure 12 shows the comparisons between the measured values for the 1-D constrained modulus based on samples and the predicted values based on eq. [42] using $\alpha_M = Q_{tn}$. The predicted values are in good agreement, but on average slightly larger than the measured values. However, sample disturbance may have made the measured values somewhat low. The largest error was for the Bothkennar site in the UK, which is a structured clay.

The number of published test sites with stiff fine-grained soils, where $Q_{tn} > 14$, are few (Cowden, UK; Madingley, UK; Piedmont, USA). The results from these three sites indicate a range for α_M from 4.5 to 6.5, compared with the suggested value of 14. In stiff clay sites, problems with sample disturbance become significant and laboratory values are almost certainly low. Mayne (2005) has shown that the short-term settlement of footings and piles can be accurately predicted using measured shear-wave velocity in a wide range of clays. As suggested in Fig. 11, as soils become stiffer, settlements are controlled more by shear stiffness than consolidation.

Although a reasonable correlation exists between predicted and measured values of the constrained modulus based on samples and laboratory testing, it is better to evaluate the proposed correlations using full-scale field tests.

To evaluate the proposed correlations further, the results from a full-scale instrumented test embankment (40 m diameter, 6.7 m height, applied load 104 kPa) constructed at a site in Treporti, Italy, were reviewed (Simonini 2004; Marchetti et al. 2006). The test embankment was constructed over a complex system of interbedded sands, silts, and silty clays with inclusions of peat that represent the Venice la-

Fig. 12. Predicted 1-D constrained modulus, M , based on cone penetration testing using $\alpha_M = Q_{tn}$ (where $Q_{tn} \leq 14$), compared with measured values based on samples and laboratory testing for soft clay sites.



goon. Instrumentation installed and monitored during loading of the embankment made it possible to back-calculate the mobilized 1-D constrained modulus in the various soil layers beneath the embankment. Details on the site conditions, embankment, and instrumentation are provided by Simonini (2004).

Marchetti et al. (2006) presented a summary of the back-calculated moduli from the embankment performance. Values of back-calculated constrained moduli (M) vary from 5 MPa in soft clay to 150 MPa in some sand layers. The high silt content of the deposits produced rapid consolidation. Piezometer readings from the instrumentation indicated no detectable excess pore pressure due to consolidation in any layer during embankment construction. The total settlement under the center of the embankment at the end of construction (i.e., after 180 days) was 360 mm. After 540 days, the total settlement was 480 mm. Hence, secondary settlement was about 25% of the total settlement at 540 days. The measurement of local vertical strains at 1 m depth intervals, down to 57 m, were obtained using high accuracy multiple extensometers. Figure 13a shows the distribution with depth of local vertical strain, ε_v , measured at the center of the embankment at the end of construction (i.e., 180 days) and clearly shows that vertical strains and settlements are mostly concentrated in the shallow soft clay layer at 1.5 to 2 m depth and in the silt layer between 8 and 17 m. A comparison between the vertical and horizontal displacements measured by inclinometers indicated that the total vertical displacements were one order of magnitude greater than the maximum horizontal displacements, i.e., soil compression occurred mostly in the vertical direction. Figure 13b shows a comparison between the back-calculated values of the 1-D constrained moduli and those predicted from the CPT using the proposed relationships. The comparison is very good, especially over the depth interval from 8 to 17 m where much of the vertical strain occurred. Since the back-calculated values were obtained over 1 m intervals, the predicted values

from the CPT (measured every 20 mm) shows more variability. The calculated end of primary 1-D settlement using the CPT estimated values for M is 400 mm compared with the measured 360 mm. The results from this instrumented case history provide a better evaluation of the proposed method than the 13 test sites (shown in Fig. 12) because the instrumented case history avoids problems associated with sample disturbance and laboratory test accuracy.

The full-scale instrumented test embankment shows that the proposed correlations between CPT and 1-D constrained moduli appear to provide good estimates, at least in normally consolidated soils.

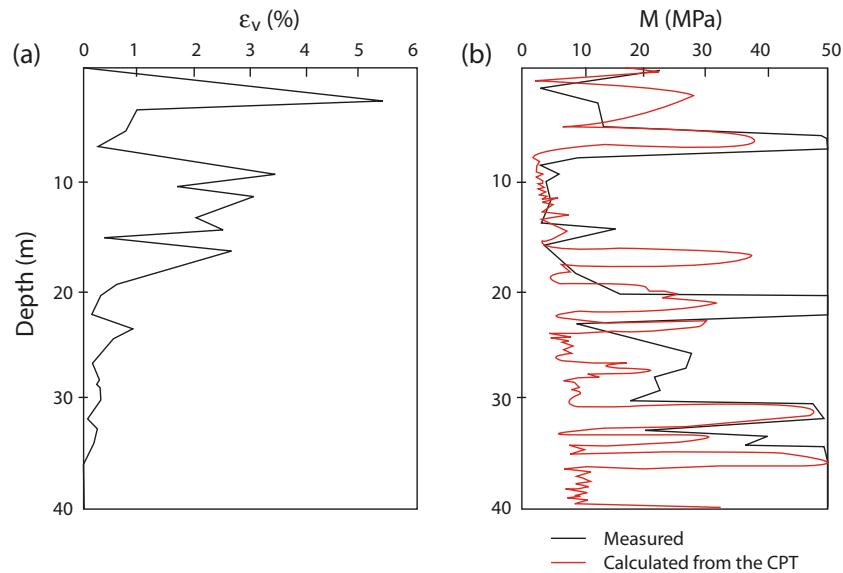
In general, estimates of the 1-D constrained modulus, M , from undrained cone penetration will be approximate. Estimates can be improved with additional information about the soil, such as plasticity index and natural moisture content, where α_M is lower for organic soils.

Summary and conclusions

The CPT has major advantages over traditional methods because it is fast, repeatable, and economical. In addition, it provides near-continuous data and has a strong theoretical background. These advantages have led to a steady increase in the use and application of the CPT in North America and many other places around the world. An update on the stress normalization for normalized cone resistance, Q_{tn} , has been provided in an effort to improve the application of the CPT for identifying soil behaviour type and various soil parameters over a wide stress range. CPT parameters can be used to provide an estimate of soil behaviour type (SBT) that may not always agree with traditional soil classifications based on grain-size distribution and soil plasticity. Hence, caution should be used in general when comparing CPT-based SBT to classifications based on samples.

As CPT data are essentially collected continuously, there can be misinterpretation when the cone is in transition at or

Fig. 13. (a) Measured distribution of vertical strains beneath full-scale instrumented test embankment at Treporti test site. (b) Comparison between measured and CPT-based predicted 1-D constrained modulus.



near an interface between soils of significantly different strength and stiffness. Recommendations are provided to identify these transition zones using the rate of change of the SBTn index, I_c , near the boundary value of 2.60.

A number of new empirical correlations have been provided to estimate various key geotechnical parameters from CPT results. Most correlations have been presented in the form of contours on the normalized soil behaviour type chart (SBTn) in terms of normalized parameters $Q_{tn}-F_r$. The correlations for soil modulus (E' and G_0) are for predominately uncemented Holocene- and Pleistocene-age soils. New correlations have also been presented to predict the 1-D constrained modulus (M) from normalized CPT parameters. The new correlations have the advantage that they apply over a wide range of soil types and compare favorably with existing correlations and with full-scale instrumented field tests. Additional full-scale field tests will aid in further evaluation and possible adjustment of the proposed correlations.

Trends in the variation of $Q_{tn}-F_r$ have been identified for changes in the OCR and soil sensitivity for fine-grained soils that can aid in the separation of these factors from CPT results.

Throughout this paper, use has been made of the normalized soil behaviour type (SBTn) chart using normalized CPT parameters $Q_{tn}-F_r$. Hence, accuracy in both q_t and f_s are important, particularly in soft fine-grained soil. Accuracy in both q_t and f_s measurements requires attention to details on unequal end-area effects, tolerance requirements, and zero-load readings. Although sleeve friction, f_s , measurements are not always as accurate as cone resistance, q_t , the proposed correlations are not overly sensitive to variations in f_s . For example, in the central region of the SBTn chart where most soils plot (see Fig. 2), a variation in f_s of $\pm 50\%$ results in a variation in I_c of less than $\pm 10\%$. Most natural soil deposits are not perfectly homogeneous and there is always some variation in measured CPT parameters. It is often useful to see the measured CPT results plotted on the SBTn charts to evaluate the natural variation. Statistical

methods can also be used to quantify the natural variability of CPT results (Lunne et al. 1997).

Many of the recommendations contained in this paper are focused on low- to moderate-risk projects where traditional methods are appropriate and where empirical interpretation tends to dominate. For projects where more advanced methods are more appropriate, the recommendations provided in this paper can be used as a screening to evaluate critical regions—zones where selective additional in situ testing and sampling maybe appropriate.

Acknowledgments

This research could not have been carried out without the support, encouragement, and input from John Gregg, Kelly Cabal, and other staff at Gregg Drilling and Testing Inc. Additional input and assistance was provided by John Ioannides and Konstantinos Lontzetidis. The comments provided by Professor P. Mayne are greatly appreciated. The sharing of data by Paul Mayne, James Schneider, Paulo Simonini, and Silvano Marchetti is also appreciated. The author is also grateful for the teaching, guidance, and encouragement provided by Professor Dick Campanella since their first collaboration over 28 years ago.

References

- Ahmadi, M.M., and Robertson, P.K. 2005. Thin layer effects on the CPT q_c measurement. *Canadian Geotechnical Journal*, **42**(5): 1302–1317. doi:10.1139/t05-036.
- Anderson, J.B., Townsend, F.C., and Rahelison, L. 2007. Load testing and settlement prediction of shallow foundation. *Journal of Geotechnical and Geoenvironmental Engineering*, **133**(12): 1494–1502. doi:10.1061/(ASCE)1090-0241(2007)133:12(1494).
- Andrus, R.D., Mohanan, N.P., Piratheepan, P., Ellis, B.S., and Holzer, T.L. 2007. Predicting shear-wave velocity from cone penetration resistance. *In Proceedings of 4th International Conference on Earthquake Geotechnical Engineering*, Thessaloniki, Greece, 25–28 June 2007. Springer, New York. Paper No. 1454.

- ASTM. 2000. Standard test method for performing electronic friction cone and piezocone penetration testing of soils. ASTM standard D5778–95. ASTM International, West Conshohocken, Pa.
- ASTM. 2006. Standard practice for classification of soils for engineering purposes (Unified Soil Classification System). ASTM standard D2487. ASTM International, West Conshohocken, Pa.
- Baldi, G., Bellotti, R., Ghionna, V.N., Jamiolkowski, M., and Lo Presti, D.F.C. 1989. Modulus of sands from CPTs and DMTs. *In Proceedings of the 12th International Conference on Soil Mechanics and Foundation Engineering*, Rio de Janeiro, Brazil, 13–18 August 1989. Balkema, Rotterdam, the Netherlands. Vol. 1, pp. 165–170.
- Bellotti, R., Ghionna, V.N., Jamiolkowski, M., and Robertson, P.K. 1989. Design parameters of cohesionless soils from in situ tests. *Transportation Research Record*, **1235**: 45–54.
- Bolton, M.D. 1986. The strength and dilatancy of sands. *Géotechnique*, **36**(1): 65–78.
- Boulanger, R.W. 2003. High overburden stress effects in liquefaction analyses. *Journal of Geotechnical and Geoenvironmental Engineering*, **129**(12): 1071–1082. doi:10.1061/(ASCE)1090-0241(2003)129:12(1071).
- Boulanger, R.W., and Idriss, I.M. 2004. State normalization of penetration resistance and the effect of overburden stress on liquefaction resistance. *In Proceedings of the 11th International Conference on Soil Dynamics and Earthquake Engineering*, Berkeley, Calif., 7–9 January 2004. American Society of Civil Engineers, Reston, Va. pp. 484–491.
- Briaud, J.L., and Gibbens, R. 1999. Behavior of five large spread footings in sand. *Journal of Geotechnical and Geoenvironmental Engineering*, **125**(9): 787–796. doi:10.1061/(ASCE)1090-0241(1999)125:9(787).
- Campanella, R.G., Gillespie, D., and Robertson, P.K. 1982. Pore pressures during cone penetration testing. *In Proceedings of the 2nd European Symposium on Penetration Testing, ESPOT II*, Amsterdam, 24–27 May 1982. Edited by A. Verruijt, F.L. Beringen, and E.H. de Leeuw. A.A. Balkema, Rotterdam, the Netherlands. pp. 507–512.
- Cetin, K.O., and Isik, N.S. 2007. Probabilistic assessment of stress normalization for CPT data. *Journal of Geotechnical and Geoenvironmental Engineering*, **133**(7): 887–897. doi:10.1061/(ASCE)1090-0241(2007)133:7(887).
- Douglas, B.J., and Olsen, R.S. 1981. Soil classification using electric cone penetrometer. *In Proceedings of the Symposium on Cone Penetration Testing and Experience*, St. Louis, Mo., 26–30 October 1981. Edited by G.M. Norris and R.D. Holtz. Geotechnical Engineering Division, American Society of Civil Engineers, New York. pp. 209–227.
- Eslaamizaad, S., and Robertson, P.K. 1996a. Seismic cone penetration test to identify cemented sands. *In Proceedings of the 49th Canadian Geotechnical Conference*, St. John's, N.L., 23–25 September 1996. Edited by J.I. Clark. Canadian Geotechnical Society, Richmond, B.C. pp. 352–360.
- Eslaamizaad, S., and Robertson, P.K. 1996b. Cone penetration test to evaluate bearing capacity of foundation in sands. *In Proceedings of the 49th Canadian Geotechnical Conference*, St. John's, N.L., 23–25 September 1996. Edited by J.I. Clark. Canadian Geotechnical Society, Richmond, B.C. pp. 429–438.
- Eslaamizaad, S., and Robertson, P.K. 1997. Evaluation of settlement of footings on sand from seismic in-situ tests. *In Proceedings of the 50th Canadian Geotechnical Conference*, Ottawa, Ont., 20–22 October 1997. BiTech Publishers, Richmond, B.C. Vol. 2, pp. 755–764.
- Eslami, A., and Fellenius, B.H. 1997. Pile Capacity by direct CPT and CPTu methods applied to 102 case histories. *Canadian Geotechnical Journal*, **34**(6): 886–898. doi:10.1139/cgj-34-6-886.
- Fahey, M., and Carter, J.P. 1993. A finite element study of the pressuremeter in sand using a nonlinear elastic plastic model. *Canadian Geotechnical Journal*, **30**(2): 348–362.
- Farrar, J.A., Torres, R., and Crutchfield, L.G. 2008. Cone penetrometer testing, Scoggins Dam, Tualatin Project, Oregon. Engineering Geology Group Bureau of Reclamation, Technical Services Center, Denver, Colo. Report No. 86–68320.
- Hardin, B.O., and Drnevich, V.P. 1972. Shear modulus and damping in soils: Design equations and curves. *Journal of the Soil Mechanics and Foundations Division*. ASCE, **98**(7): 667–692.
- Hegazy, Y.A., and Mayne, P.W. 1995. Statistical correlations between VS and cone penetration data for different soil types. *In Proceedings of the International Symposium on Cone Penetration Testing, CPT '95*, Linköping, Sweden, 4–5 October 1995. Swedish Geotechnical Society, Linköping, Sweden. Vol. 2, pp. 173–178.
- Hight, D., and Leroueil, S. 2003. Characterization of soils for engineering purposes. *In Characterization and engineering properties of natural soils*, Vol. 1. Swets and Sitlinger, Lisse, the Netherlands. pp. 255–360.
- Idriss, I.M., and Boulanger, R.W. 2004. Semi-empirical procedures for evaluating liquefaction potential during earthquakes. *In Proceedings of the 11th International Conference on Soil Dynamics and Earthquake Engineering*, Berkeley, Calif., 7–9 January 2004. American Society of Civil Engineers, Reston, Va. pp. 32–56.
- ISSMFE. 1999. International reference test procedure for cone penetration test (CPT). Report of the International Society for Soil Mechanics and Foundation Engineering (ISSMFE) Technical Committee on Penetration Testing of Soils, TC 16. Swedish Geotechnical Institute, Linköping, Sweden. Information 7, pp. 6–16.
- Jamiolkowski, M., and Robertson, P.K. 1988. Future trends for penetration testing. *In Penetration testing in the UK*. Thomas Telford, London. pp. 321–342.
- Jamiolkowski, M., Ladd, C.C., Germaine, J.T., and Lancellotta, R. 1985. New developments in field and laboratory testing of soils. *In Proceedings of the 11th International Conference on Soil Mechanics and Foundation Engineering*, San Francisco, Calif., 12–16 August 1985. A.A. Balkema, Rotterdam, the Netherlands. Vol. 1, pp. 57–153.
- Janbu, N. 1963. Soil compressibility as determined by oedometer and triaxial tests. *In Proceedings of the 2nd European Conference on Soil Mechanics and Foundation Engineering*, Wiesbaden, Germany, 15–18 October 1963. Deutsche Gesellschaft für Erd- und Grundbau, Essen, Germany. Vol. 1, pp. 19–25.
- Jefferies, M.G., and Been, K. 2006. *Soil liquefaction – A critical state approach*. Taylor & Francis Group, London and New York. ISBN 0-419-16170-8.
- Jefferies, M.G., and Davies, M.O. 1991. Soil classification by the cone penetration test: Discussion. *Canadian Geotechnical Journal*, **28**(1): 173–176. doi:10.1139/t91-023.
- Jefferies, M.G., and Davies, M.P. 1993. Use of CPTU to estimate equivalent SPT N_{60} . *Geotechnical Testing Journal*, **16**(4): 458–468. doi:10.1520/GTJ10286J.
- Kulhawy, F.H., and Mayne, P.H. 1990. Manual on estimating soil properties for foundation design. Electric Power Research Institute (EPRI), Palo Alto, Calif. Report EL-6800.
- Long, M. 2008. Design parameters from in situ tests in soft ground — recent developments. *In Geotechnical and Geophysical Site Characterization, Proceedings of the Third International Conference on Site Characterization*, Taipei, Taiwan, 1–4 April

2008. *Edited by* A.-B. Huang and P.W. Mayne. Taylor & Francis Group, London. pp. 89–116
- Lunne, T., and Andersen, K.H. 2007. Soft clay shear strength parameters for deepwater geotechnical design. *In Proceedings of the 6th International Conference on Offshore Site Investigation and Geotechnics*, London, 11–13 September 2007. Society for Underwater Technology, London. pp. 151–176.
- Lunne, T., Eidsmoen, T., Gillespie, D., and Howland, J.D. 1986. Laboratory and field evaluation on cone penetrometers. *In Proceedings of ASCE Specialty Conference In Situ'86: Use of In Situ Tests in Geotechnical Engineering*, Blacksburg, Va., 23–25 June 1986. Geotechnical Special Publication No. 6. *Edited by* S.P. Clemence. American Society of Civil Engineers (ASCE), New York. pp. 714–729.
- Lunne, T., Robertson, P.K., and Powell, J.J.M. 1997. Cone penetration testing in geotechnical practice. Blackie Academic, EF Spon/Routledge, New York.
- Marchetti, S., Monaco, P., Calabrese, M., and Totani, G. 2006. Comparison of moduli determined by DMT and backfigured from local strain measurements under a 40 m diameter circular test load in the Venice Area. *In Proceedings of the 2nd International Flat Dilatometer Conference*, Washington, D.C., 2–5 April 2006. pp. 220–230. Insitu, Va.
- Mayne, P.W. 2000. Enhanced geotechnical site characterization by seismic piezocone penetration tests. *In Proceedings of the 4th International Geotechnical Conference, Invited Lecture, Cairo, Egypt. Edited by* M.M. Abdel-Rahman, S.W. Agaiby, and M.A. Fam. Soil Mechanics and Foundation Research Laboratory, Faculty of Engineering, Cairo University, Egypt. pp. 95–120.
- Mayne, P.W. 2005. Integrated ground behavior: In-situ and lab tests. *In Proceedings of the International Symposium on Deformation Characteristics of Geomaterials*, Lyon, France, 22–24 September 2005. Taylor & Francis Group, London. Vol. 2, pp. 155–177.
- Mayne, P.W. 2007. Cone penetration testing: A synthesis of highway practice. Project 20-5. Transportation Research Board, Washington, D.C. NCHRP synthesis 368.
- Mayne, P.W. 2008. Piezocone profiling of clays for maritime site investigations. *In Proceedings of the 11th Baltic Sea Geotechnical Conference*, Gdansk, Poland, 15–18 September 2008. International Society for Soil Mechanics and Geotechnical Engineering, London. pp. 151–178.
- Molle, J. 2005. The accuracy of the interpretation of CPT-based soil classification methods in soft soils. M.Sc. thesis, Section for Engineering Geology, Department of Applied Earth Sciences, Delft University of Technology, Delft, the Netherlands. Report No. 242, Report AES/IG/05–25.
- Monaco, P., Totani, G., and Calabrese, M. 2006. DMT-predicted vs. observed settlements: A review of the available experience. *In Proceedings of the 2nd International Flat Dilatometer Conference*, Washington D.C., April 2006. pp. 244–252.
- Moss, R.E.S., Seed, R.B., and Olsen, R.S. 2006. Normalizing the CPT for overburden stress. *Journal of Geotechnical and Geoenvironmental Engineering*, **132**(3): 378–387. doi:10.1061/(ASCE)1090-0241(2006)132:3(378).
- Ohta, H., Nishihara, A., and Morita, Y. 1985. Undrained stability of K_0 -consolidated clays. *In Proceedings of 11th International Conference on Soil Mechanics and Foundation Engineering (ICSMFE)*, San Francisco, Calif., 12–16 August 1985 A.A. Balkema, Rotterdam, the Netherlands. Vol. 2, pp. 613–661.
- Olsen, R.S., and Malone, P.G. 1988. Soil classification and site characterization using the cone penetrometer test. *In Proceedings of the First International Symposium on Penetration Testing, ISOPT-1*, Orlando, Fla., 20–24 March 1988. *Edited by* J.A. De Ruiter. Balkema, Rotterdam, the Netherlands. Vol. 2, pp. 887–893.
- Olsen, R.S., and Mitchell, J.K. 1995. CPT stress normalization and prediction of soil classification. *In Proceedings of the International Symposium on Cone Penetration Testing*, Linköping, Sweden, 4–5 October 1995. Vol. 2. Swedish Geotechnical Society, Linköping, Sweden. pp. 257–262.
- Plewes, H.D., Davies, M.P., and Jefferies, M.G. 1992. CPT based screening procedure for evaluating liquefaction susceptibility. *In Proceedings of the 45th Canadian Geotechnical Conference*, Toronto, Ont., 26–28 October 1992. BiTech Publishers Ltd., Richmond, B.C. pp. 41–49.
- Rad, N.S., and Lunne, T. 1986. Correlations between piezocone results and laboratory soil properties. Norwegian Geotechnical Institute, Oslo, Norway. pp. 306–317. Report 52155.
- Robertson, P.K. 1990. Soil classification using the cone penetration test. *Canadian Geotechnical Journal*, **27**(1): 151–158. doi:10.1139/t90-014.
- Robertson, P.K. 1995. Penetrometer testing – Session IV: Moderators report. *In Proceedings of the Conference on Advances in Site Investigation Practice*, London, 30–31 March 1995. Thomas Telford, London.
- Robertson, P.K. 1998. Risk-based site investigation. *Geotechnical News*, **16**(3): 45–47.
- Robertson, P.K. 2009. CPT–DMT correlations. *Journal of Geotechnical and Geoenvironmental Engineering*, **135**(11): 1762–1771. doi:10.1061/(ASCE)GT.1943-5606.0000119.
- Robertson, P.K., and Campanella, R.G. 1983a. Interpretation of cone penetration tests. Part I: sand. *Canadian Geotechnical Journal*, **20**(4): 718–733. doi:10.1139/t83-078.
- Robertson, P.K., and Campanella, R.G. 1983b. Interpretation of cone penetration tests. Part II: clay. *Canadian Geotechnical Journal*, **20**(4): 734–745. doi:10.1139/t83-079.
- Robertson, P.K., and Campanella, R.G. 1989. Design manual for use of CPT and CPTU. The University of British Columbia, Vancouver, B.C.
- Robertson, P.K., and Wride, C.E. 1998. Evaluating cyclic liquefaction potential using the cone penetration test. *Canadian Geotechnical Journal*, **35**(3): 442–459. doi:10.1139/cgj-35-3-442.
- Robertson, P.K., Campanella, R.G., Gillespie, D., and Greig, J. 1986a. Use of piezometer cone data. *In Proceedings of ASCE Specialty Conference In Situ'86: Use of In Situ Tests in Geotechnical Engineering*, Blacksburg, Va., 23–25 June 1986. Geotechnical Special Publication No. 6. *Edited by* S.P. Clemence. American Society of Civil Engineers (ASCE), New York. pp. 1263–1280.
- Robertson, P.K., Campanella, R.G., Gillespie, D., and Rice, A. 1986b. Seismic CPT to measure in-situ shear wave velocity. *Journal of the Geotechnical Engineering Division, ASCE*, **112**(8): 791–803. doi:10.1061/(ASCE)0733-9410(1986)112:8(791).
- Robertson, P.K., Woeller, D.J., and Finn, W.D.L. 1992. Seismic cone penetration test for evaluating liquefaction potential. *Canadian Geotechnical Journal*, **29**(4): 686–695. doi:10.1139/t92-075.
- Sanglerat, G. 1972. The penetrometer and soil exploration. Elsevier Science Ltd., Amsterdam, the Netherlands.
- Schnaid, F. 2005. Geocharacterization and Engineering properties of natural soils by in-situ tests. *In Proceedings of the 16th International Conference on Soil Mechanics and Geotechnical Engineering*, Osaka, Japan, 12–16 September 2005. Millpress, Rotterdam, the Netherlands. Vol. 1, pp. 3–45.
- Schneider, J.A., McGillivray, A.V., and Mayne, P.W. 2004. Evaluation of SCPTU intra-correlations at sand sites in the Lower Mississippi River valley, USA. *In Proceedings of the 2nd Inter-*

- national Conference on Site Characterization, ISC'2, Geotechnical and Geophysical Site Characterization, Porto, Portugal, 19–22 September 2004. Millpress, Rotterdam, the Netherlands. pp. 1003–1010.
- Seed, H.B., and Idriss, I.M. 1970. Soil moduli and damping factors for dynamics response analysis. University of California, Berkeley, Calif. Report No. EERC 70–10.
- Shuttle, D.A., and Cunning, J. 2007. Liquefaction potential of silts from CPTu. *Canadian Geotechnical Journal*, **44**(1): 1–19. doi:10.1139/T06-086.
- Simonini, P. 2004. Characterization of Venice lagoon silts from in-situ tests and performance of a test embankment. *In Proceedings of the 2nd International Conference on Site Characterization, ISC'2, Geotechnical and Geophysical Site Characterization, Porto, Portugal, 19–22 September 2004. Millpress, Rotterdam, the Netherlands. Vol. 1, pp. 187–207.*
- Vesic, A.S., and Clough, G.W. 1968. Behaviour of granular materials under high stresses. *Journal of the Soil Mechanics and Foundations Division, ASCE*, **94**(SM3): 313–326.
- Wride, C.E., Robertson, P.K., Biggar, K.W., Campanella, R.G., Hofmann, B.A., Hughes, J.M.O., Küpper, A., and Woeller, D.J. 2000. Interpretation of in situ test results from the CANLEX sites. *Canadian Geotechnical Journal*, **37**(3): 505–529. doi:10.1139/T00-044.
- Wroth, C.P. 1984. The interpretation of in-situ soil tests: Rankine Lecture. *Géotechnique*, **34**(4): 449–489.
- Zhang, Z., and Tumay, M.T. 1999. Statistical to fuzzy approach toward CPT soil classification. *Journal of Geotechnical and Geoenvironmental Engineering*, **125**(3): 179–186. doi:10.1061/(ASCE)1090-0241(1999)125:3(179).
- Zhang, G., Robertson, P.K., and Brachman, R.W.I. 2002. Estimating liquefaction-induced ground settlements from CPT for level ground. *Canadian Geotechnical Journal*, **39**(5): 1168–1180. doi:10.1139/t02-047.